The 13th Symposium on Polar Science

15 – 18 November 2022

National Institute of Polar Research
Research Organization of Information and Systems

Session OG

Polar Geosciences

Program and Abstracts

Conveners
Jun'ichi Okuno, and Yuichi Aoyama (NIPR)

【OG】Polar Geosciences

Scopes

This session covers research topics from the fields of geology, mineralogy, geomorphology, quaternary research, geodesy, and geophysics.

Conveners : **Jun'ichi Okuno, and Yuichi Aoyama (NIPR)**

Real-time Oral presentations (09:55 – 12:00, 13:30 – 15:10)

Date: Wed. 16 November

Chair: Tomokazu Hokada (NIPR)			
	9:55 - 10:00	Opening	Jun'ichi Okuno (PEDSC, NIPR)
OGo1	**10:00 - 10:20**	First report of ultrahigh-temperature sapphirine granulites from the Mesoproterozoic Irumide Belt in southern Africa	*Wakabayashi So (University of Tsukuba), Tsunogae Toshiaki (University of Tsukuba), Nyirongo Mzee Wandembo (University of Tsukuba)
OGo2	**10:20 - 10:40**	Metamorphism and geochronology of metapelites and felsic orthogneisses from the Dete-Kamativi Inlier, NW Zimbabwe: Implications for a Rodinia-related intracratonic orogen in Southern Africa	*Mandingaisa Prince (Tsukuba University), Tsunogae Toshiaki (Tsukuba University), Tsutsumi Yukiyasu (National Museum of Nature and Science, Tsukuba)
OGo3	**10:40 - 11:00**	The pressure-temperature conditions of high-grade pelitic gneisses in the Dai Loc Complex, Truong Son Belt, central Vietnam	*Kitano Ippei (Hokkaido University), Bui Thi Sinh Vuong (Vietnam Academy of Science and Technology), Osanai Yasuhito (Kyushu University), Nakano Nobuhiko (Kyushu University), Pham Binh (Vietnam Institute of Geosciences and Mineral Resources), Hokada Tomokazu (National Institute of Polar Research)
OGo4	**11:00 - 11:20**	Structural geology and tectonic evolution of the Western Dharwar Craton: some new insights into the Archean tectonics of the Dharwar Craton	*Lakshmanan Sreehari (Shimane University), Toyoshima Tsuyoshi (Niigata University), Madhusoodhan Satish-Kumar (Niigata University), Ueda Hayato (Niigata University)
OGo5	**11:20 - 11:40**	Report of the 10th Student Himalayan Field Exercise Tour and Recruit for the 11th Tour.	*Yoshida Masaru (Gondwana Institite for Geology and Environment), Paudel Mukunda (Tribhuvan University, Nepal), Arita Kazunori (Hokkaido University), Sakai Tetsuya (Shimane University), Upreti Bishal Nath (Nepal Academy of Science and Technology)
OGo6	**11:40 - 12:00**	Composition of Oil Fractions in the Upper Horizons of Arctic Tundra Soils with Different Duration of Pollution	*Bikmullina Zarina (Hokkaido University), Zavgorodnyaa Yulia (Moscow State University)
Lunch			
Chair: Kenji Horie (NIPR)			
OGo7	**13:30 - 13:50**	Metamorphic rocks from Chijire Rocks in the eastern part of the Prince Olav Coast, East Antarctica	*Baba Sotaro (University of the Ryukyus), Kagashima Shin-ich (Yamagata University), Nakano Nobuhiko (Kyushu University), Hokada Tomokazu (NIPR)

OGo8	**13:50 - 14:10**	The Western Rayner Complex – connection between Dronning Maud Land and Enderby Land, East Antarctica	*Hokada Tomokazu (NIPR & SOKENDAI), Baba Sotaro (University of the Ryukyus), Kamei Atsushi (Shimane University), Kitano Ippei (Hokkaido University), Horie Kenji (NIPR & SOKENDAI), Takehara Mami (NIPR)
OGo9	**14:10 - 14:30**	Carbon isotopes as a proxy in tracing carbon mobility in the continental crust of East Antarctica: Implications for carbon geodynamic cycle in orogenic belts	*Satish-Kumar M. (Niigata Univeristy)
OGo10	**14:30 - 14:50**	Multiple fluid infiltration during post-peak metamorphism in southern Perlebandet, Sør Rondane Mountains, East Antarctica	*Higashino Fumiko (Kyoto University), Kawakami Tetsuo (Kyoto University), Adachi Tatsuro (Kyushu University), Uno Masaoki (Tohoku University)
OGo11	**14:50 - 15:10**	Sulfide mineralogy and whole-rock sulfur isotope composition of high-grade metamorphic rocks from the Sør Rondane Mountains, East Antarctica	*Kawakami Tetsuo (Kyoto University), Satish-Kumar M. (Niigata University), Mitsubori Tokuya (Niigata University), Silpa Ammini Sasidharan (Niigata University, Shimane University)

Real-time Poster presentations (15:30 – 17:30)

Date: Wed. 16 November

OGp1	Infiltration of K-Cl-rich fluid in mafic granulite from Austhovde	*Hiroi Yoshikuni (Chiba University and NIPR), Hokada Tomokazu (NIPR), Adachi Tatsuro (Kyushu University), Kamei Atsushi (Shimane University), Shiraishi Kazuyuki (NIPR), Motoyoshi Yoichi (NIPR)
OGp2	Series of fluid activities during brittle-viscous shear deformation in amphibolite on the southern side of the Main Shear Zone, Ketelersbreen, Sør Rondane Mountains, East Antarctica	*Mindaleva Diana (Tohoku University), Uno Masaoki (Tohoku University), Higashino Fumiko (Kyoto University), Adachi Tatsuro (Kyushu University), Kawakami Tetsuo (Kyoto University), Tsuchiya Noriyoshi (Tohoku University)
OGp3	Metamorphic condition and age of a pelitic gneiss from Niban-nishi Rock of Niban Rock in the Lü tzow-Holm Complex, East Antarctica	*Mori Yuki (JASRI/SPring-8), Hokada Tomokazu (NIPR), Miyamoto Tomoharu (Kyushu University), Ikeda Takeshi (Kyushu University)
OGp4	Zircon geochronology and geochemistry of syenites in the Yamato Mountains, East Antarctica	*Horie Kenji (NIPR & SOKENDAI), Takehara Mami (NIPR), Hokada Tomokazu (NIPR & SOKENDAI)
OGp5	Multichronology of Harvey Nunatak, Napier Complex, East Antarctica	*Takehara Mami (NIPR), Horie Kenji (NIPR & SOKENDAI), Hokada Tomokazu (NIPR & SOKENDAI)?
OGp6	Dependence of GIA-induced gravity change in Antarctica on viscoelastic Earth structure	*Irie Yoshiya (NIPR), Okuno Jun'ichi (NIPR, SOKENDAI), Ishiwa Takeshige (NIPR, SOKENDAI), Doi Koichiro (NIPR, SOKENDAI), Fukuda Yoichi (NIPR, Kyoto University)
OGp7	A study of the relationship between rapid flow velocity deceleration events of Shirase Glacier, East Antarctica, and the surrounding bathymetry	*Ohkawa Shotaro (SOKENDAI), Doi Koichiro (NIPR, SOKENDAI), Aoyama Yuichi, (NIPR,SOKENDAI)
OGp8	Mid-Holocene deglacial history along the Lützow-Holm Bay verified by the geodetic observations and GIA modeling	Hattori Akihisa (SOKENDAI), *Okuno Jun'ichi (NIPR, ROIS & SOKENDAI), Doi Koichiro (NIPR & SOKENDAI), Aoyama Yuichi (NIPR & SOKENDAI)

First report of ultrahigh-temperature sapphirine granulites from the Mesoproterozoic Irumide Belt in southern Africa

So Wakabayashi [1], Toshiaki Tsunogae [1] and Mzee Wandembo Nyirongo[1]
[1]*University of Tsukuba*

The dominant lithologies of the Paleoo- to Neoproterozoic basement rocks in Malawi exhibit semi-pelitic biotite gneiss with intercalated felsic to intermediate orthogneisses (e.g., charnockite and biotite-hornblende gneiss), metabasites (amphibolite and mafic granulite), and metasediments (e.g., khondalite, quartzo-feldspathic gneiss, calc-silicate rock, quartzite, and marbles) (e.g., Hanson, 2003; Tsunogae et al., 2021). The central part of Malawi corresponds to the boundary region of the Irumide Belt (1.1-1.0 Ga) and the Southern Irumide Belt (600-550 Ma) (e.g., De Waele et al., 2006; Johnson et al., 2006; Karmaker and Schenk, 2016). Therefore, the region is regarded as key to understanding multiple collision events during Paleo- to Neoproterozoic. However, available petrological and geochronological date from central Malawi is still limited and are not sufficient for predicting tectonic evolution of this region and allow the regional correlation of orogenic events. Therefore, we evaluated pelitic gneiss samples collected from Jenda area in the Irumide Belt situated between the Bangweulu Block to the north and the Kalahari Craton to the south, and obtained new petrological, geothermobarometric, and geochronological date from the samples.

Based on detailed petrographic and mineral chemical studies, we report here for the first time, the occurrence of sapphirine + quartz assemblage in textural equilibrium from a pelitic gneiss from the Irumide Belt. The pelitic gneiss is dark brownish gray in color and shows strong foliation. The foliation is defined by alternation of leucocratic band (which is rich in quartzs and feldspar) and melanocratic band (which is rich in Fe-Ti oxide, sillimanite, and cordierite). The rock is composed of K-feldspar, plagioclase, quartz, cordierite, sillimanite, biotite, spinel, orthopyroxene and sapphirine, with accessory monazite and zircon. Mineral equilibrium modeling has been done on the pelitic gneiss in the system NCKFMASHTO and the results gave peak *P-T* condition of >887ºC and 6.6 kbar for the sapphirine + quartz stability, suggesting ultrahigh-temperature metamorphism. In situ dating of monazite grains occurring in the gneiss revealed that the high-grade metamorphism took place at ca. 1.1 Ga, which coincides with the timing of the amalgamation of supercontinent Rodinia (e.g., De Waele et al., 2006; Johnson et al., 2006; Karmaker and Schenk, 2016).

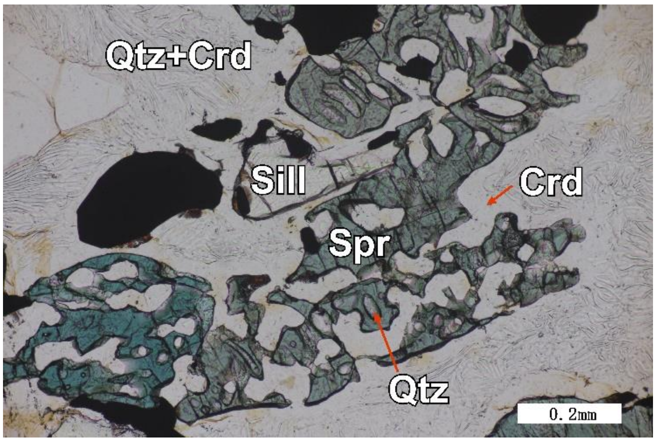

References

De Waele, B., Kampunzu, A.B., Mapani, B.S.E., Tembo, F., 2006. The mesoproterozoic irumide belt of Zambia. Journal of African Earth Sciences, 46, 36–70.

Johnson, S.P., De Waele, B., Liyungu, K.A., 2006. U-Pb sensitive high-resolution ion microprobe (SHRIMP) zircon geochronology of granitoid rocks in eastern Zambia: terrane subdivision of the Mesoproterozoic Southern Irumide Belt. Tectonics, 25, TC6004.

Karmaker, S., Schenk, V., 2016. Mesoproterozoic UHT metamorphism in the Southern Irumide Belt, Chipata, Zambia: Petrology and in situ monazite dating. Precambrian Research, 275, 332-356.
Hanson, R.E., 2003. Proterozoic geochronology and tectonic evolution of southern Africa. Geological Society, London, Special Publications, 206, 427–463.
Tsunogae, T., Uthup, S., Nyirongo, M.W., Takahashi, K., Rahman, M.S., Liu, Q., Takamura, Y., Tsutsumi, Y., 2021. Neoproterozoic crustal growth in southern Malawi: New insights from petrology, geochemistry, and U-Pb zircon geochronology, and Implications for the Kalahari Craton-Congo Craton amalgamation. Precambrian Research, 352, 106007.

Metamorphism and geochronology of metapelites and felsic orthogneisses from the Dete-Kamativi Inlier, NW Zimbabwe: Implications for a Rodinia-related intracratonic orogen in Southern Africa

Prince Mandingaisa [1,2], Toshiaki Tsunogae [3,4], Yukiyasu Tsutsumi [5]

[1] *Degree Program in Geoscience, University of Tsukuba, Ibaraki 305-8572, Japan*
[2] *Department of Geology, University of Zimbabwe, Mt. Pleasant, Harare, Zimbabwe*
[3] *Faculty of Life and Environmental Sciences, University of Tsukuba, Ibaraki 305-8572, Japan*
[4] *Department of Geology, University of Johannesburg, Auckland Park 2006, South Africa*
[5] *Department of Geology and Paleontology, National Museum of Nature and Science, Ibaraki 305-0005, Japan*

The Magondi Belt, which outcrops on the western part of the Zimbabwe Craton has been regarded as a Paleoproterozoic orogen formed by the collision of the Zimbabwe Craton and an unknown continental block (terra incognita) during the ca. 2.0 Ga Magondi orogeny (e.g., Master et al., 2010). The Dete-Kamativi Inlier (DKI) situated approximately 200 km west-southwest of the main Magondi Belt has been regarded as an extension of the Magondi Belt because of remarkable lithological correspondence, together with the similarities in terms of ages (e.g., Master, 1991). Here, we report new geochronological data for pelitic schists and a felsic orthogneiss from the DKI using monazites (CHIME method) and zircons (LA-ICP-MS analysis) and discuss the tectonic evolution of the region. Geochronological analysis of zircon grains inherent in a felsic orthogneiss from the Kamativi area revealed a magmatic and metamorphic age of 2279 ± 25 Ma and 2020 ± 28 Ma, respectively. Similar Paleoproterozoic ages of ca. 2.1–1.8 Ga were also obtained from subhedral and rounded monazite grains in the pelitic schists. In contrast, irregular-shaped monazite intergrown with biotite in a different pelitic schist gave three latest Mesoproterozoic isochron ages of 1196 ± 37 Ma, 1143 ± 32 Ma, and 1070 ± 25 Ma, suggesting a long-lived (>120 million years) thermal event with several monazite-growing stages. Consistent isochron ages of 1062 ± 41 Ma and 1061 ± 26 Ma were obtained from monazites in the felsic orthogneiss and metapelite samples from an adjacent region. Garnet-biotite geothermometers revealed a peak P–T condition of 520–600 °C and 1.5–2.5 kbar for the peak mineral assemblage in the garnet-andalusite-biotite-cordierite-bearing pelitic schist with 1196-1070 Ma metamorphic ages, suggesting low-pressure amphibolite-facies metamorphism. The condition is lower than that obtained from the hornblende-plagioclase geothermometry of amphibolites (>700 °C) from the southwest part of the DKI, which probably corresponds to an earlier (ca. 2.0 Ga) high-grade metamorphic condition. The youngest thermal event, 994–982 Ma, from monazite rim in a mylonitic orthogneiss might correspond to the timing of later heating related to deformation. The latest Mesoproterozoic (1.2–1.1 Ga) amphibolite-facies metamorphism was likely associated with an intracratonic orogeny related to the activity of broadly coeval orogenic events (e.g., Namaqualand orogen) related to the amalgamation of the Rodinia supercontinent (e.g., Li et al., 2008).

References

Li, Z.X., Bogdanova, S., Collins, A.S., Davidson, A., De Waele, B., Ernst, R.E., Fitzsimons, I.C.W., Fuck, R.A., Gladkochub, D.P., Jacobs, J. and Karlstrom, K.E., 2008. Assembly, configuration, and break-up history of Rodinia: a synthesis. Precambrian research, 160(1-2), pp.179-210.

Master, S., 1991. Stratigraphy, tectonic setting, and mineralization of the early Proterozoic Magondi Supergroup, Zimbabwe: a review. Economic Geology Research Unit, University of the Witwatersrand.

Master, S., Bekker, A. and Hofmann, A., 2010. A review of the stratigraphy and geological setting of the Paleoproterozoic Magondi Supergroup, Zimbabwe–Type locality for the Lomagundi carbon isotope excursion. Precambrian Research, 182(4), pp.254-273

The pressure-temperature conditions of high-grade pelitic gneisses in the Dai Loc Complex, Truong Son Belt, central Vietnam

Ippei Kitano[1], Vuong Bui Thi Sinh[2, 3], Yasuhito Osanai[3], Nobuhiko Nakano[3], Binh Pham[4] and Tomokazu Hokada[5, 6]
[1]*Hokkaido University*
[2]*Vietnam Academy of Science and Technology*
[3]*Kyushu University*
[4]*Vietnam Institute of Geosciences and Mineral Resources*
[5]*National Institute of Polar Research*
[6]*Department of Polar Science, The Graduate University for Advanvced Studies (SOKENDAI)*

The Dai Loc Complex is a Devonian–Silurian granitoid complex located at the southmost Truong Son Belt in central Vietnam along the Tam Ky–Phuoc Son suture zone. The suture zone corresponds to the boundary between the Truong Son Belt and Kontum Massif which is a Ordovician–Silurian and Permo–Triassic plutono–metamorphic complex (e.g., Nakano et al., 2013). The Dai Loc Complex is composed of granodiorite, granite and aplite with I- and S-type affinities (e.g., Hieu et al., 2016; Jiang et al., 2020). The gneissose or augen structures are well developed in most of the Dai Loc granitoids (e.g., Jiang et al., 2020). These granitoids intrudes into the Cambrian–Ordovician A Vuong Formation which consists of weakly metamorphosed sandstone, schist, and quartzite (Faure et al., 2018). Recently, the occurrences of high-grade pelitic gneisses in the Dai Loc Complex have been reported (Osanai et al., 2018; Bui et al., 2022). The pelitic gneisses are characterized by migmatitic structure associated with euhedral Crd-bearing leucosome, and mineral assemblages of Grt porphyroblast with textural zoning (inclusion-rich core, inclusion-free mantle, and dusty rim), Crd, and Bt with/without minor Spl, Sil, Ky, and St (Osanai et al., 2018; Bui et al., 2022). Bui et al. (2022) reported Zrn U–Pb ages of *ca.* 440–430 Ma obtained from metamorphic Zrn domain including rare Sil and *ca.* 2500–500 Ma as detrital Zrn ages. They suggested a low pressure (LP) / high temperature (HT) stage with the coexistence of Grt (core and mantle) + Crd + Bt ± Spl ± Sil at *ca.* 440–430 Ma and subsequent isobaric cooling which produced Grt dusty rim and Ky + Bt ± St aggregate after Crd. However, the metamorphic conditions of pelitic gneisses in the Dai Loc Complex, which give a critical clue to reveal the tectonic evolution of the southern part of the Truong Son Belt, haven't been constrained yet. Therefore, this study reports the pressure (*P*)–temperature (*T*) conditions of two Grt–Crd–Bt gneisses dated by Bui et al. (2022) (samples 73102I and 73103F) and an Opx-bearing Grt–Crd–Bt gneiss (sample 73102B) we newly identified (Fig. 1), and discuss the tectonic implication.

The Grt in these samples chemically can be divided into high-Ca core and low-Ca rim (Fig. 2) that correspond to the core and/or mantle, and rim described by Bui et al. (2022), respectively. The high-Ca core (X_{grs} = 0.022–0.041) shows the normal zoning with decrease in Mn, slight increase or almost homogenity of Mg toward its margin in 73102I (Fig. 2) and 73102B, while that of Grt in 73103F shows opposite zoning pattern. The low-Ca rim (X_{grs} = 0.001–0.015) has lower Mn and higher Mg contents than the core or Mg contents similar to the core (Fig. 2). The Grt core includes Bt, Als (Sil?), Pl, Qz, Ilm, Rt, and Ap. Inclusions in Grt rim are too tiny to be identified. Opx (X_{Mg} = 0.376–0.387, Al_2O_3 = 2.90–3.17 wt%) in 73102B occurs in the leucosome as a subhedral porphyroblast surrounded by Cum and Bt + Qz (Fig. 1). Bt is present in the matrix (X_{Mg} = 0.424–0.654, TiO_2 = 0.00–5.97 wt%) or inside Grt and Crd (X_{Mg} = 0.423–0.642, TiO_2 = 0.29–6.40 wt%). The Bt in the matrix is overgrown by fine-grained Bt ± Qz or partly replaced by low-Ca dusty Grt. Anhedral and euhedral Crd can be recognized in the melanosome (X_{Mg} = 0.602–0.761) and leucosome (X_{Mg} = 0.671–0.753 (73103F)), respectively. The former includes anhedral to subhedral green Spl (X_{Mg} = 0.137–0.164 (73102B), 0.189–0.254 (73102I), 0.255–0.270 (73103F)) in association with Crn and/or Dsp. The Crd grains are replaced by Ky + Bt ± St (X_{Mg} = 0.149–0.164 (73102B), 0.220–0.260 (73103F)) ± Ged (X_{Mg} = 0.363–0.378 (73102B), 0.427–0.485 (73102I, 73103F)) ± low-Ca dusty Grt ± Qz. Pl lamellae of the mesoperthite in the matrix are enriched in Na (X_{An} = 0.005–0.047), while the Pl inclusions in the Grt (X_{An} = 0.089, 0.207) of 73102I and Pl in the leucosome of 73103F (X_{An} = 0.192–0.264) represent relatively higher anorthite contents. Opaque phases are Ilm in 73102B and 73102I, and Py in 73103F.

The application of the Grt–Bt, Grt–Crd, and Grt–Opx geothermometers, and Grt–Bt–Pl–Qz, Grt–Rt–Als–Ilm–Qz, and Grt–Bt–Als–Qz geobarometers indicates the *P*–*T* conditions on prograde, peak and retrograde stages as follows:

・Prograde stage (Grt + Bt + Pl + Qz ± Ilm ± Als(Sil?) ± Rt):
T = 560–600 ℃ (73102B), *P* = 4.1–5.6 kbar and *T* = 600–670 ℃ (73102I)
・Peak stage (Grt + Crd + Spl + Bt + Pl + Afs + Qz ± Ilm ± Opx ± Als(Sil?) ± Rt ± Py):
T = 800–950 ℃ (73102B), *P* = 6.0–8.5 kbar and *T* = 730–800 ℃ (73102I), *P* = 6.0–7.7 kbar and *T* = 730–840 ℃ (73103F)
・Retrograde stage (Grt + Ky + Ged + Bt ± St + Pl + Afs + Qz ± Ilm ± Py):

P = 7.5–9.2 kbar and T = 670–700 °C (73102B), P = 6.5–7.8 kbar and T = 580–630 °C (73102I), P = 6.5–7.5 kbar and T = 580–620 °C (73103F)

Additionally, the Ti-in-Grt geothermometer for Ilm-bearing samples yields T = 900–950 °C (73102B) and 850–900 °C (73102I).

The results suggest the counter-clockwise P–T paths with peak granulite-facies condition and subsequent isobaric cooling upto epidote amphibolite- to amphibolite-facies condition for pelitic gneisses in the Dai Loc Complex. Their peak P–T conditions are well comparable with those of the Ordovician–Silurian metamorphic rocks in the eastern Kannack Complex and western Ngoc Linh Complex of the Kontum Massif. The results of this study support Bui et al. (2022) who inferred the isobaric cooling process for the Dai Loc pelitic gneisses and the Ordovician–Silurian LP/HT metamorphism triggered by subduction-related arc magmatism between the Kontum Massif and Dai Loc Complex. The core of Grt in the 73102B and 73102I preserves the prograde zoning of Mn without homogenization by the diffusion under the granulite-facies HT condition. It may represent that the Dai Loc pelitic gneisses experienced the rapid burying and heating followed by quick cooling process. The post-peak isobaric cooling may be explained by the horizontal movement of pelitic gneisses together with the Dai Loc granitoids in the arc crust to get away from the heat source. Thus, the metamorphic evolution of pelitic gneisses in the Dai Loc Complex possibly indicates the development of the arc-trench system involving the arc magmatism and LP/HT metamorphism during Ordovician–Silurian in the southern Truong Son Belt.

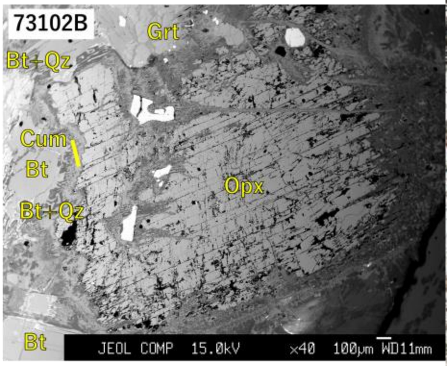

Fig. 1. The occurrence of Opx in sample 73102B.

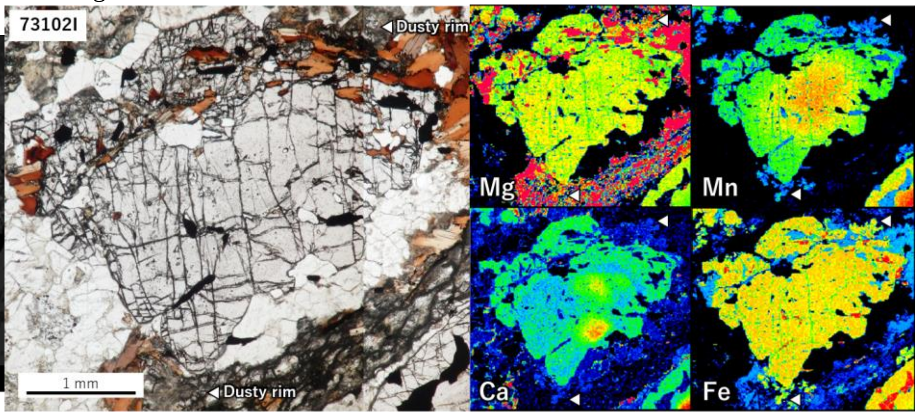

Fig. 2. The occurrence and X-ray mapping of Grt in sample 73102I. The white triangle marks indicate the locations of representative dusty rim of Grt.

Abbreviation: Afs, alkali feldspar; Als, aluminosilicate; Ap, apatite; Bt, biotite; Crd, cordierite; Crn, corundum; Cum, cummingtonite; Dsp, diaspore; Ged, gedrite; Grt, garnet; Ilm, ilmenite; Ky, kyanite; Opx, orthopyroxene; Pl, plagioclase; Py, pyrite; Qz, quartz; Rt, rutile; Spl, spinel; Sil, sillimanite; St, staurolite; Zrn, zircon

References

Bui, T.S.V., Osanai, Y., Nakano, N., Kitano, I., Adachi, T., Tran, T.A. and Binh, P., Petrology and zircon U–Pb geochronology of pelitic gneisses and granitoids from the Dai Loc Complex in the Truong Son Belt, Vietnam: implication for the Silurian magmatic-metamorphic event. Journal of Asian Earth Sciences, 226, 105070, 2022.

Faure, M., Nguyen, V.V., Hoai, L.T.T. and Lepvrier, C., Early Paleozoic or Early-Middle Triassic collision between the South China and Indochina Blocks: The controversy resolved? Structural insights from the Kon Tum massif (Central Vietnam). Journal of Asian Earth Sciences, 166, 162–180, 2018.

Hieu, P.T., Dung, N.T., Thuy, N.T.B., Minh, N.T. and Minh, P., U-Pb ages and Hf isotopic composition of zircon and bulk rock geochemistry of the Dai Loc granitoid complex in Kontum massif: Implications for Early Paleozoic crustal evolution in Central Vietnam. Journal of Mineralogical and Petrological Sciences, 111 (5), 326–336, 2016.

Jiang, W., Yu, J.-H., Wang, X., Griffin, W.L., Pham, T.H., Nguyen, D.L. and Wang, F., Early Paleozoic magmatism in northern Kontum Massif, Central Vietnam: Insights into tectonic evolution of the eastern Indochina Block. Lithos 376–377, 105750, 2020.

Nakano, N., Osanai, Y., Owada, M., Nam, T.N., Charusiri, P. and Khamphavong, K., Tectonic evolution of high-grade metamorphic terranes in central Vietnam: Constraints from large-scale monazite geochronology. Journal of Asian Earth Sciences, 73, 520–539, 2013.

Osanai, Y., Nakano, N., Binh, P. and Bui, T.S.V., Excursion Guide Post-symposium excursion FE06 (Kontum Massif). The fifteenth regional congress on geology, mineral and energy resources of Southeast Asia (GEOSEA XV), 2018.

Structural geology and tectonic evolution of the Western Dharwar Craton: some new insights into the Archean tectonics of the Dharwar Craton

L. Sreehari[1], T. Toyoshima[2], M. Satish-Kumar[2], H. Ueda[2]
[1]*Department of earth science, Shimane University, Matsue, Japan*
[2]*Department of Geology, Niigata University, Niigata, Japan*

The Dharwar Craton (DC) is the largest Archean craton in India. Based on lithology, age and geochemistry DC is divided into Western Dharwar Craton (WDC) and Eastern Dharwar Craton (EDC). The WDC is older and has wider schist belts than EDC and preserved key geological and structural features associated with evolutionary history of the DC. The WDC consists of two volcanosedimentary sequences older Sargur Group (>3.0 Ga) and younger Dharwar Supergroup (<3.0 Ga). In the EDC schist belts are comparatively narrow and intruded by younger (~2.5 Ga) granites. In this study we present detailed structural and stratigraphic relations across different schist belts in the Dc giving preference to the schist belts in the WDC. Especially in the Chitradurga Schist Belt (CSB), Bababudan Schist Belt (BSB) and Shimoga Schist Belt (SSB). Six stages of deformation events were identified from the study area; among those two events (D2 and D3) were regional-scale deformations. D2 event represent reverse faults and upright folds while D3 event is strike-slip sinistral fault. Schist belts are dominated by volcano-sedimentary rocks and boarded by granitic gneisses. The contact between schist belts and basement gneiss is marked by the presence of conglomerate with oversized quartzite pebbles in amphibole rich matrix. In some locations the conglomerate is oligomict with quartz pebbles in sandy matrix. The boundary between schist belts also dominated by D2 reverse faults. sedimentary rocks in the schist belts show dominance of shallow marine indicators and slump folding structures. Most of the rock formation in the WDC is folded during D2 event and the intensity of the folding increases from the west to east. Tightly folded sequences are present in the CSB, that is the eastern margin of WDC. Unfolding of the layers show that the schist belts are narrow, short-lived basins typically resembling aborted-rift settings in the Phanerozoic. Folded layers seem to be sandwiched between reverse faults (D2) in the margin of the schist belts, in total represents a fold-and-thrust belt. The overall structural architecture of WDC suggest that the schist belts in probably represent multiple stages of failed rifts later amalgamated during regional-scale deformation. Present day structures in the schist belts of the DC possibly represent an inverted failed rift basin. Sediments and volcanic rocks deposited in basin formed by rifted granitic basement and several immature basins were formed in different parts of the WDC.

Another regional-scale deformation event is strike-slip sinistral shear (D3). Gadag–Mandya Shear Zone (GMSZ) present in the eastern margin of the WDC is part of this event. GMSZ is considered as a terrain boundary by in previous research, but our detailed fieldwork shows that it is difficult to find a broad shear zone in the eastern margin of the WDC. This implies that the actual terrain boundary between cratonic units will be in the east probably near Kolar schist belt. An interesting unit of conglomerate unit identified from the eastern margin of the Kolar schist belt has horizontal bedding and almost unaffected by later phase of deformations. We suppose this conglomerate unit with mafic and felsic clast and silicious to volcaniclastic matrix represent the youngest event in the DC. So, the youngest event in the DC probably not compression, later stage extensional events occurred near the Kolar schist belts and those regions probably represent the terrain boundary of the cratonic units. These statements should be supported by both geochemical and geochronological analysis.

Our investigations points that the CSB or other schist belts in the WDC is not an accretionary complex or not preserved remnants of an oceanic crust. Schist belts in the WDC represents multiple stages of failed rifts. Terrain boundary between cratonic units probably lies more towards the eastern margin of the Kolar schist belt. Our findings are majorly based on field and structural investigations, so to support this more evidence from geochronology and geochemistry of the key rock units are necessary.

Report of the 10th Student Himalayan Field Exercise Tour and Recruit for the 11th tour

Yoshida, M[*, **]. Paudel, M.[**], Arita, K.[***], Sakai, T[****]. and Upreti, B.N[*****].

[*]*Gondwana Institute for Geology and Environment and Tribhuvan University(Em, Professor),* [**]*Department of Geology, Tri-Chandra Campus, Tribhuvan University,* [***]*Hokkaido University Museum,* [****]*Interdisciplinary Science and Engineering, Shimane University,* [*****]*Nepal Academy of Science and Technology*

The Student Himalayan Field Exercise Tour (SHET) started in 2012 and in 2022, the 10th SHET was carried out (details are given in Yoshida, 2022). The SHET aimed to show students the full N-S section of the Himalayan Orogen (Fig. 1) to let students feel the dynamic crustal processes in the field. The details of the SHET program are given on the SHET home page (2022).

The 10th SHET was successfully carried out for 17 days (Japan-Neal-Japan) in March 2022, the details are given by Yoshida (2022). The advertisement of the SHET-10 started in May 2021 and 11 students including a Chinese student who was funded by the IAGR registered by January 2022, however, 6 among them cancelled in February due to the COVID-19 pandemic problem. On the 20th February, two weeks before the departure of the tour, the Foreign Ministry of Japan identified Nepal as the grade 3 of the danger of COVID-19 infection indicating [Advise not to visit Nepal with any reasons]. However for Nepal, the number of newly affected per 100000 persons that is regarded to be the basic barometer of the danger of infection was one 56th of Japan. Information collected from several sources in Nepal also showed that there is practically no problem in Nepal. Considering those informations, we decided to conduct the tour.

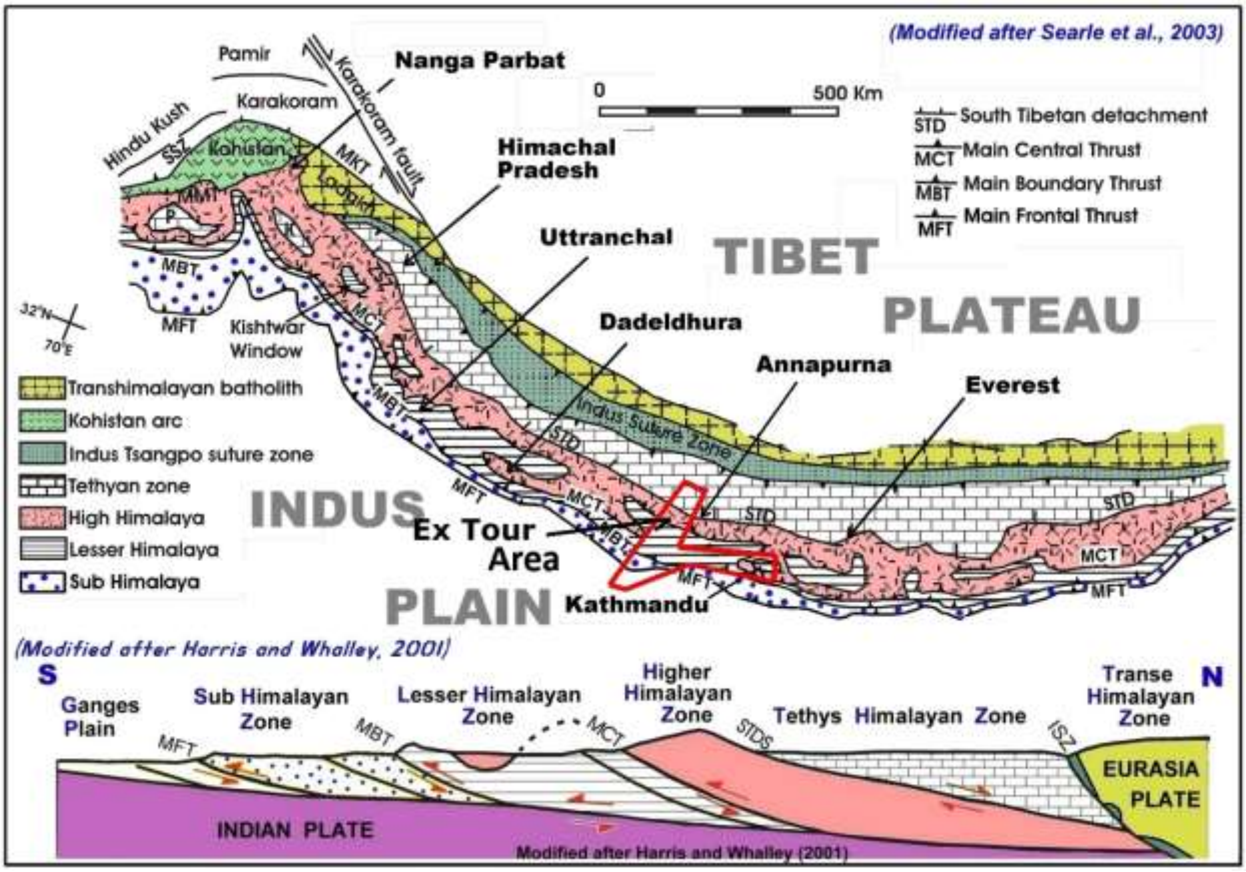

Fig. 1. Geologic outline of the Himalayan Orogen and area of the SHET-10 study

On the 3rd of March, the SHET-10 team departed Japan. On the 6th, the SHET-10 team including 5 Japanese and Nepali students and a Japanese and a Nepali leaders/teachers of the tour departed Kathmandu by a chartered bus for the field excursion. The tour course included a full N-S traverse of the Himalayan Orogen in the west-central Nepal from Mustang north of Annapurna to Terai through Kali Gandaki and Tinau Khola, the course having been same as that during the SHET-1 to SHET-9.

The weather was fine and participants met no health problems throughout the tour and thus could enjoy the full fascination of the Himalayan geology in the field. Before and after the field tour, the team had pre- and post- field tour seminars and city tours in Kathmandu with many Nepali students. On the 18th March the Japanese team left Kathmandu for Japan. The SHET-10 thus completed successfully. The only problems in conducting the tour were to clear regulations and rules related to the Covid-19 pandemic at immigration of and return to countries, although they were anyway of no fundamental problem. An outline of the SHET-10 including highlight views of the field observation will be displayed at the presentation.

The SHET-11 is scheduled to be conducted in March 2023 as usual and recruiting leaflet will be displayed in the presentation. Although the COVIX-19 pandemic may or may not be at that time, we believe that we can clear any problems related with this issue. Only the problem for the SHET-11 is the high price of the airfare and other expenses that have been created by the Covid-19 pandemic problems. We have started a crowd funding project (SHET-CF, 2022) to reduce the participation fee of students for the SHET-11.

References

SHET homepage, 2022, Student Himalayan Field Exercise site, in the GIGE homepage, http://www.gondwanainst.org/geotours/Studentfieldex_index.htm

SHET-CF, 2022, Let's student to study in the Himalaya! Program – Requesting your collaboration to the crowd funding. www.gondwanainst.org/shet-cf

Yoshida, M., 2022 (ed.), Traversing the Himalayan Orogen 2022--A Record of the 10th Student Himalayan Field Exercise Tour in March 2022 (in Japanese and English). Field Science Publishers, Hashimoto, 191 pages. (https://www.data-box.jp/pdir/8d74595d276149a99b6ffac68d9b6391).

Composition of Oil Fractions in the Upper Horizons of Arctic Tundra Soils with Different Duration of Pollution

Zarina Bikmullina[1], Yulia Zavgorodnyaa[2]
[1]*Hokkaido University, Sapporo, Japan,* [2]*Soil Science Faculty, Moscow State University, Moscow, Russia*

Petrochemical contamination of soils is a challenging issue, especially for subpolar regions where bio- and chemical degradation rate of pollutants is low (Bento et al., 2005). High-molecular-weight oil compounds, such as resins and asphaltenes, are less degradable and, thus, may affect the soil even many years after pollution termination; however, these compounds are usually ignored in environmental standardization and assessment of environment quality.

In this study, changes of oil fractions composition in upper horizons (0-20 cm) of contaminated Arctic tundra soils near the Yareiyskoe oilfield (Yamalo-Nenets Autonomous Okrug, Russia) were investigated. Samples were taken from areas near suspended wells. We assumed that the date of suspension could be considered as a date of intensive pollution termination.

An analytical method of extraction and fractionation of petroleum from contaminated soils is proposed. It successfully implements the separation of soil extracts into 3 fractions. F1 (non-polar, mostly consist of aliphatic HCs, cycloalkanes, mono-, bi- and triaromatics; eluted by hexane), and F2 (slightly polar, consist of oxidized products of HCs; eluted by chloroform) were analyzed by GC-MS. Benzene/methanol (1:1 v/v) extracted F3 was expected to include compounds such as resins and asphaltenes, and the analysis of was performed by LC-MS ((Herod et al., 2007).

Fraction composition shows changes for easily degradable compounds: relative abundance of linear alkanes decreased, whereas saturated polycyclanes shown higher percentage (fig. 1).

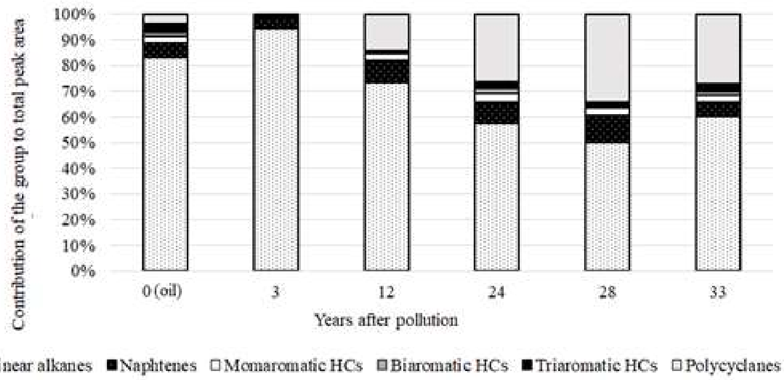

Fig. 1. Ratio of groups identified in F1

In F2, relative abundance of aliphatic-derived oxidized products increases; precursors/products ratio decreases up to 20 times (fig. 2). As contamination period rises, contribution of oxidized aliphatics becomes less, whereas oxi-PAHs start to prevail.

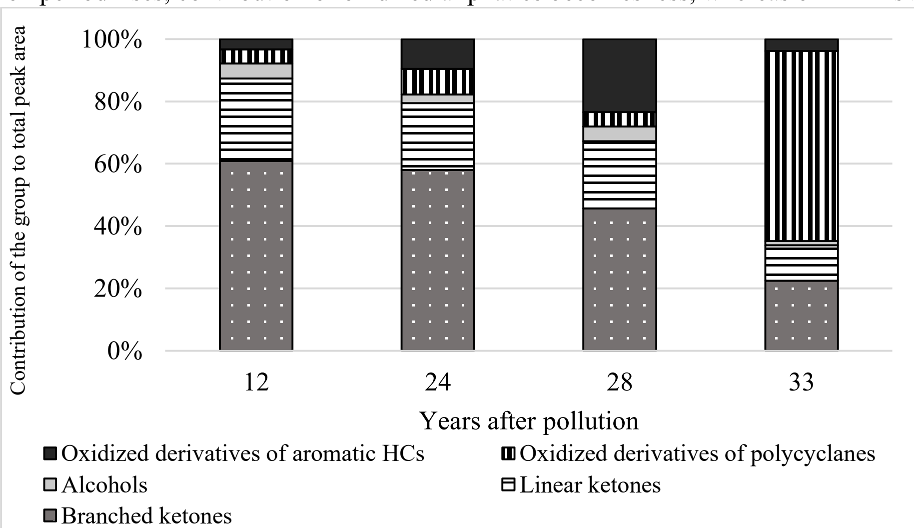

Fig. 2. Ratio of groups identified in F2

F3 analysis shows similarity of compounds' molecular weights and molecular formulae in samples with different period after pollution. The possible interpretation of these data is that total degradation of maltenes fraction in Arctic tundra soils requires much more than 30 years.

References

Bento, F.M., Camargo, F.A.O., Okeke, B.C., Frankenberger, W.T., 2005. Comparative bioremediation of soils contaminated with diesel oil by natural attenuation, biostimulation and bioaugmentation. Bioresour. Technol. 96, 1049–1055.

Herod, A. A.; Bartle, K. D.; Kandiyoti, R. Characterization of Heavy Hydrocarbons by Chromatographic and Mass Spectrometric Methods: An Overview. Energy Fuels 2007, 21, 2176−2203.

Metamorphic rocks from Chijire Rocks in the eastern part of the Prince Olav Coast, East Antarctica

Sotaro Baba[1], Shin-ich Kagashima[2], Nobuhiko Nakano[3] and Tomokazu Hokada[4]

[1]*University of the Ryukyus*
[2]*Yamagata University*
[3]*Kyushu University*
[4]*National Institute of Polar Research*

The Lützow-Holm complex, East Antarctica, predominates the area from the eastern part of Droning Maud Land (35°E) to the western part of Enderby Land (45°E) and is the Ediacaran-Cambrian mobile belt (Hiroi et al., 1991; Shiraishi et al., 1994; 2003). The Japanese Antarctic Research Expedition (JARE) surveyed this complex and compiled 27 geological maps. However, numerous small exposures have not been explored, and their geological constituents are unresolved. The geological survey team of the 63rd JARE (2021-2022) conducted a geological survey of unknown outcrops of the Lützow-Holm complex and outcrops that have not been surveyed in recent years. We will introduce the geological overview, characteristics of constituent lithology, and metamorphic conditions of the unexplored Chijire Rocks.

The Chijire Rocks are located about 160 km west of Syowa Station. Two rock exposures are distributed to the east and west of the small glacier. In this survey, we investigated small exposure in the west, about 1km east-west, and about 0.5 km north-south. Basement rocks show an isoclinic structure with a northwest-southeast trend and dip to the south at 65-80 degrees. Structurally from lower to upper levels: biotite-garnet gneiss, hornblende-garnet gneiss/amphibolite, biotite-garnet gneiss, layered gneisses, hornblende-biotite gneiss are recognized, and are intruded by pegmatite and minor basalt. Layered gneisses consist of alternating layers of large garnet-bearing amphibolite, garnet-gedrite/anthophyllite gneiss, garnet-biotite gneiss, and felsic gneisses, which develop a layered structure well. The Garnet-biotite-sillimanite gneiss was found in the biotite-garnet gneiss close to the boundary between layered gneisses and biotite-garnet gneiss. Since this rock contains staurolite, it is beneficial for estimating metamorphism's temperature and pressure conditions. We selected significant rocks from each lithofacies and clarified their mineral and chemical compositions.

This presentation discusses the differences in the precursor rocks of these gneisses inferred from the mineral chemical composition. In addition, we compare the chemical composition and occurrence of the staurolite with those of the neighboring outcrops and consider the difference in formation conditions.

References

Hiroi, Y., Shiraishi, K., Motoyoshi, Y., Late Proterozoic paired metamorphic complexes in East Antarctica, with special reference to the tectonic significance of ultramafic rocks. In: Thomson, M.R.A., Crame, J.A., Thomson, J.W. (Eds.), Geological Evolution of Antarctica. Cambridge University Press, pp. 83–87, 1991.

Shiraishi, K., Ellis, D.J., Hiroi, Y., Fanning, C.M., Motoyoshi, Y. Nakai, Y., Cambrian orogenic belt in east Antarctica and Sri Lanka: implications for Gondwana assembly. J. Geol. 102, 47–65, 1994.

Shiraishi, K., Hokada, T., Fanning, C.M., Misawa, K., Motoyoshi, Y., 2003. Timing of thermal events in eastern Dronning Maud Land, East Antarctica. Polar Geosci. 16, 2003.

The Western Rayner Complex – connection between Dronning Maud Land and Enderby Land, East Antarctica

Tomokazu Hokada[1,2], Sotaro Baba[3], Atsushi Kamei[4], Ippei Kitano[5], Kenji Horie[1,2] and Mami Takehara[1]
[1] *National Institute of Polar Research*
[2] *Department of Polar Science, The Graduate University for Advanced Studies (SOKENDAI)*
[3] *University of the Ryukyus*
[4] *Shimane University*
[5] *The Hokkaido University Museum, Hokkaido University*

The Western Rayner Complex is located in the key connection area among three distinct geologic units Archaean Napier Complex to the northeast, Mesoproterozoic Rayner Complex to the southeast and the Neoproterozoic-Cambiran Lützow-Holm Complex to the west. The age of the Western Rayner Complex has been well constrained as 550-520 Ma metamorphism and ~780Ma or c.2500 Ma protoliths (Shiraishi et al., 1997, 2008). The area can be subdivided into the charnockite-dominant western part (Vechernyaya Suite; ~780 Ma) and the mixed protolith eastern part (Forefinger Suite; c.2500 Ma). UHT peak metamorphic conditions and a clockwise P-T trajectory have been estimated for pelitic rocks from Forefinger Point (Harley et al., 1990; Motoyoshi et al., 1995).

According to the recent SHRIMP zircon studies on the neighboring Rayner Complex (Horie et al., 2016) and the geologic field studies (JARE-58; Hokada, Baba, Kamei, Kitano), the Rayner Glacier is considered as the boundary between the ~900 Ma Rayner and the ~500 Ma Western Rayner Complexes. We have investigated high–T metamorphic rocks from 3 nunataks in Enderby land, East Antarctica. Two unnamed nunataks "1702-24-2 Nunatak" and "1702-24-3 Nunatak" are located on both sides across the Rayner Glacier, the inferred boundary between the Rayner Complex and the Western Rayner Complex. Quartzo-feldspathic Bt gneiss and Cpx-Hb-bearing mafic-intermediate gneisses are distributed in 1702-24-2 nunatak. Quartzo-feldspathic Grt-Bt or Bt gneisses and Opx-bearing mafic granulite occur in 1702-24-3 Nunatak. Another outcrop, Point Widdows is located in western part of the Western Rayner Complex, and is predominated by massive quartzo-feldspathic Opx gneiss (charnockite) with local hydration zones. This presentation summarizes the current understanding of the Western Rayner Complex, and the surrounding areas of this part of Antarctica.

References

Harley, S.L., Hensen, B.J., Heraton, J.W., Two-stage decompression in orthopyroxene-sillimanite granulites from the Forefinger Point, Enderby Land, Antarctica. Implications for the evolution of the Archaean Napier Complex. Journal of Metamorphic Geology, 8, 591-613, 1990.

Horie, K., Hokada, T., Motoyoshi, Y., Shiraishi, K., Hiroi, Y., Takehara, M., U-Pb zircon geochronology in the western part of the Rayner Complex, East Antarctica. Journal of Mineralogical and Petrological Sciences, 111, 104-117, 2016.

Motoyoshi, Y., Ishikawa, M. And Fraser, G.L., Sapphirine-bearing silica-undersaturated granulites from Forefinger Point, Enderby Land, East Antarctica: evidence for a clock-wise P-T path ! Proceedings of the NIPR Symposium on Antarctic Geosciences, 8, 121-129, 1995.

Shiraishi, K., Ellis, D.J., Fanning, C.M., Hiroi, Y., Kagami, H. and Motoyoshi, Y., Reexamination of the metamorphic and protolith ages of the Rayner complex, Antarctica: Evidence for the Cambrian (Pan-African) regional metamorphic event. In: Ricci, C.A. (ed.) The Antarctic Region: Geological Evolution and Processes. Terra Antartica, Sienna, 79–88, 1997.

Shiraishi, K., Dunkley, D.J., Hokada, T., Fanning, C.M., Kagami, H., Hamamoto, T., Geochronological constraints on the Late Proterozoic to Cambrian crustal evolution of eastern Dronning Maud Land, East Antarctica: a synthesis of SHRIMP U-Pb age and Nd model age data. In: Satish-Kumar, M. et al. (Eds.), Geodynamic Evolution of East Antarctica: A Key to the East-West Gondwana Connection. Geological Society, London, Special Publication, 308, 21-67, 2008.

Carbon isotopes as a proxy in tracing carbon mobility in the continental crust of East Antarctica: Implications for carbon geodynamic cycle in orogenic belts

M. Satish-Kumar[1]

[1]*Department of Geology, Faculty of Science, Niigata University, 2-8050 Ikarashi, Nishi-ku, Niigata 950-2181, Niigata Japan*

Organic carbon and carbonate carbon are two important reservoirs that control the carbon geodynamic cycle at convergent margins during plate subduction, arc magmatism and continent building processes. The movement of carbon through different reservoirs in the Earth relating to the global tectonic activities especially, in the convergent margins, is key in understanding the carbon geodynamic cycle. A recent study on Earth's tectonic carbon conveyor belt quantified the fluxes into and out of all reservoirs in the deep oceanic carbon cycle over past 250 million years and provided boundary conditions for future carbon cycle models (Muller et al., 2022). However, a quantitative evaluation of carbon geodynamic cycle at the continental collision zones is not yet carried out. Here, I present a comprehensive synthesis on the different forms of carbon, its movement among various reservoirs in the Lützow-Holm Complex (LHC) of East Antarctica and uses carbon isotopic composition as a proxy to identify the movement of carbon during orogenesis. The results suggest that large volumes of carbon can be stored in the middle to lower continental crust in the form of graphitic carbon and carbonate carbon, as long-term sinks.

Sedimentary carbonate rocks trapped in orogenic belts are of key importance, since they remain stable as metacarbonate rocks for longer time scales, even after subjected to varying degrees of metamorphism up to ultra-high temperature conditions (e.g., Satish-Kumar et al., 2021 and references therein). Metacarbonate rocks are prominent rock units in orogenic belts and form an important carbon reservoir in the continental crust. They occur in large volumes in the Lützow-Holm Complex (LHC) in East Antarctica, which forms a part of the Neoproterozoic to early Paleozoic East African Antarctic Orogeny (Shiraishi et al., 1994; Satish-Kumar et al., 2008a, 2013), with different suits of rocks with varying protolith history, as proposed in a recent subdivision by Dunkley et al. (2020). The LHC, located along the Prince Olav, Prince Herald and Soya coasts (~400 km), in East Antarctica, comprises of a thick pile of metamorphosed pelitic and carbonate rocks associated with granitic and mafic meta-igneous rocks. Deposition of thick sedimentary sequences is considered to have occurred in a continental marginal tectonic setting (Satish-Kumar *et al.,* 2008b, 2010). The closure of Mozambique ocean during the Gondwana amalgamation resulted in extensive accretion of sedimentary sequences, where abundant dolomitic marbles are particularly seen in the Skalleviksshalsen Suite (Satish-Kumar et al., 2008b). Metamorphism during continental collision has resulted in the formation of calc-silicate minerals by decarbonation reactions, which can release a fraction of carbon as CO_2. However, the volume of CO_2 released is limited as evidenced by the preservation of sedimentary carbonate isotopic compositions (($\delta^{13}C$ values near to 0‰; Satish-Kumar and Wada, 2000; Satish-Kumar *et al.,* 1998, 2008b). A comprehensive compilation of carbon and oxygen isotopic composition of orogenic metacarbonate rocks indicate that there is only a minimal effect of decarbonation and CO_2 release from carbonate rocks during orogenesis (Satish-Kumar et al., 2021). Thus, pure carbonate rocks in orogenic belts can act as a long-term sink for carbon.

Graphite, the purest form of carbon in collisional orogenic belts, is an important reservoir of carbon in continental crust. Graphite occurs in a variety of rock types in the LHC. Based on the mode of occurrence they were classified into several types, disseminate flakes in gneissic rocks, coarse aggregates in leucosomes, graphite concentration in lithological contacts and as monomineralic graphite veins. At the Skallvikshalsen locality in the LHC, all forms of carbon are observed in a single outcrop scale and thereby movement of carbon within the crust could be traced clearly. Disseminated graphite in pelitic gneisses have the lowest carbon isotopic composition ($\delta^{13}C$ values as low as -25‰, Fig. 1), suggesting sedimentary biogenic signatures, however those in metacarbonate rocks have equilibrated with carbonate during high temperature metamorphism to heavier values ($\delta^{13}C$ values in the range

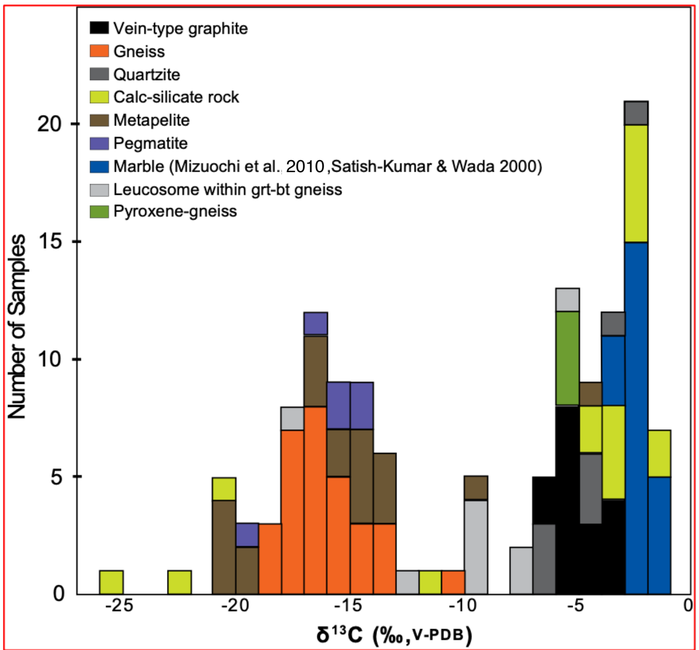

Figure 1. Distribution of carbon isotopic composition of graphite in various rock types in the Lützow-Holm Complex, East Antarctica.

between-3‰ to -1‰, Fig. 1). Carbon isotopic composition of graphite and associated metacarbonate rocks suggest that they are consistent with graphite precipitation from CO_2 fluids locally released through decarbonation reactions. Formation of vein type of graphite is significant, since the veins have penetrated into the felsic gneiss from metacarbonate rocks, suggesting a possible origin from CO_2 fluids released by decarbonation reactions during skarn formation at contact zones.

Coarse-grained graphite is also observed to concentrate in leucosomes in the migmatized meta-pelitic rocks at the Rundvågshetta occurrence. During the high-temperature metamorphism and partial melting of graphite-bearing rocks, graphite decomposes to form COH fluids, part of which, especially the lighter isotope-bearing fluids are supposed to have escaped the system causing a shift toward heavier values ($\delta^{13}C$ values in the range between-18‰ to -10‰, Fig. 1). Based on the field, textural and carbon isotope evidence from Rundvågshetta, biotite dehydration melting of graphite-bearing rocks caused the dissolution of graphite and during melt crystallization graphite has reprecipitated, resulting in carbon remobilization and carbon isotope reorganization, similar to the model suggested by Satish-Kumar et al. (2011). Thus, carbon is recycled and retained as graphite in the continental crust during high-grade metamorphism and anatexis, though its isotopic composition can be considerably modified.

In summary, a comprehensive study of carbon isotopic composition of graphite and carbonate rocks in the Lützow-Holm Complex, East Antarctica has thus revealed the role of recycling of carbon within the continental crust during orogenesis. A detailed synopsis on the movement of carbon from a carbon isotope perspective will be presented to understand the role of carbonate and graphite as "long-term sinks" of carbon during orogenesis.

References

Dunkley, D.J., Hokada, T., Shiraishi, K., Hiroi, Y., Nogi, Y. and Motoyoshi, Y., Geological subdivision of the Lützow–Holm Complex in East Antarctica: From the Neoarchean to the Neoproterozoic. Polar Science, 26, 100606. https://doi.org/10.1016/j.polar.2020.100606, 2020.

Mizuochi, H., Satish-Kumar, M., Motoyoshi, Y. and Michibayashi, K., Exsolution of dolomite and application of calcite-dolomite solvus geothermometry in high-grade marbles: an example from Skallevikshalsen, East Antarctica, Journal of Metamorphic Geology, 28, 509-526, 2010.

Muller, R.D., Mather, B., Dutkiewicz, A., Keller, T., Merdith, A., Gonzalez, C.M., Gorczyk, W. and Zahirovic, S., Evolution of Earth's tectonic carbon conveyor belt. Nature, 605, 629–639, 2022.

Satish-Kumar, M. and Wada, H., Carbon isotopic equilibrium between calcite and graphite in Skallen marbles, East Antarctica: Evidence for preservation of peak metamorphic temperatures. Chem. Geol., 166, 172–183, 2000.

Satish-Kumar, M., Hermann, J., Miyamoto, T. and Osanai, Y., Fingerprinting a multistage metamorphic fluid–rock history: Evidence from grain scale Sr, O and C isotopic and trace element variations in high-grade marbles from East Antarctica. Lithos, 114, 217–228, 2010.

Satish-Kumar, M., Hokada, T., Owada, M., Osanai, Y. and Shiraishi, K., Neoproterozoic orogens amalgamating East Gondwana: Did they cross each other? Precambrian Res., 234, 1–7, 2013.

Satish-Kumar, M., Hokada, T., Kawakami, T. and Dunkley, D.J. Geosciences Research in East Antarctica: Present status and future perspectives. In: Satish-Kumar, M., Motoyoshi, Y., Osanai, Y., Hiroi, Y. & Shiraishi, K. (eds.) "Geodynamic evolution of East Antarctica: a key to the East–West Gondwana connection" Geological Society of London, Special Publications, 308, 1-21. 2008a.

Satish-Kumar, M., Miyamoto, T., Hermann, J., Kagami, H., Osanai, Y. and Motoyoshi, Y., Pre-metamorphic carbon, oxygen and strontium isotope signature of high-grade marbles from the Lützow Holm Complex, East Antarctica: apparent age constraints of carbonate deposition. In: Satish-Kumar, M., Motoyoshi, Y., Osanai, Y., Hiroi, Y. & Shiraishi, K. (eds.) "Geodynamic evolution of East Antarctica: a key to the East–West Gondwana connection". Geological Society of London, Special Publications, 308, 147-164. 2008b.

Satish-Kumar, M., Shirakawa, M., Imura, A., Otsuji-Makino, N., Imanaka-Nohara, R., Malaviarachchi, S.P.K., Fitzsimons, I.C.W., Sajeev, K., Grantham, G.H., Windley, B.F., Hokada, T., Takahashi, T., Shimoda, G. and Goto, K.T., A geochemical and isotopic perspective on tectonic setting and depositional environment of Precambrian meta-carbonate rocks in collisional orogenic belts. Gondwana Res., DOI: 10.1016/j.gr.2021.03.013, 2021.

Satish-Kumar, M., Yoshida, M., Wada, H., Niitsuma, N. and Santosh, M., Fluid flow along microfractures in calcite from a marble from East Antarctica: Evidence from gigantic (21per mil) oxygen isotopic zonation. Geology, 26, 251–254, 1998.

Satish-Kumar, M., Yurimoto, H., Itoh, S. and Cesare B., Carbon isotope anatomy of a single graphite crystal in a metapelitic migmatite revealed by high-spatial resolution SIMS analysis Contrib. Mineral. Petrol., 162, 821–834, 2011.

Shiraishi, K., Ellis, D.J., Hiroi, Y., Fanning, C.M., Motoyoshi, Y. and Nakai, Y., Cambrian orogenic belt in East Antarctica and Sri Lanka: implication for Gondwana assembly. Journal of Geology, 102, 47-65, 1994.

Multiple fluid infiltration during post-peak metamorphism in southern Perlebandet, Sør Rondane Mountains, East Antarctica

Fumiko Higashino[1], Tetsuo Kawakami[1], Tatsuro Adachi[2] and Masaoki Uno[3]
[1]*Kyoto University,* [2]*Kyushu University and* [3]*Tohoku University*

The Sør Rondane Mountains (SRM), East Antarctica are dominated by high-temperature metamorphic rocks and granitoids (e.g., Shiraishi et al., 1997). There are controversial arguments about the tectonic process around the SRM; Jacobs et al. (2003) considers that the SRM are the part of collision zone between East and West Gondwana during the East African-Antarctic Orogeny, whereas Meert (2003) suggests the crossing points of the East African Orogen and the Kuunga Orogen are located around the Dronning Maud Land. The field distribution of Cl-rich minerals and their formation mechanisms have been studied in the SRM (e.g., Higashino et al., 2019; Kawakami et al., 2017; Uno et al., 2017). The previous studies report Cl-rich biotite and hornblende, which are possibly evidence of saline fluid activity, are observed in felsic and mafic gneisses along large-scale shear zones and major tectonic boundaries over 200 km (Higashino et al., 2013, 2019). The Cl-bearing fluid activity is recognized during prograde to post-peak metamorphisms (Higashino et al., 2013, 2019; Kawakami et al., 2017). The NaCl-CO_2-H_2O system is often assumed as fluid composition in the crust (e.g., Liebscher and Heinrich, 2007). However, CO_2-bearing fluid is not reported in the SRM, whereas Cl-bearing fluid has been examined in detail.

Perlebandet is ~10 km long nunataks located at the westernmost part of the SRM, where granites are exposed in the structurally lower part of the metamorphic rocks. Perlebandet was categorized to the NE-terrane which exhibits a clockwise pressure-temperature (*P*-*T*) path (Osanai et al., 2013). However, Mieth et al. (2014) proposes that Perlebandet is part of the SW-terrane based on the magnetic survey. The counter-clockwise *P-T* path based on petrochronological constraint from northern Perlebandet by Kawakami et al. (2017) supports this interpretation. Kawakami et al. (2017) also reports Cl-rich fluid infiltration during prograde stage. So far, all previous studies in Perlebandet reporting the *P-T* conditions, zircon U-Pb ages, and CHIME monazite ages dealt with samples collected from northern part of Perlebandet (Asami et. al., 2005; Shiraishi et al., 2008; Kawakami et al., 2017). This study deals with pelitic gneisses collected from southern part of nunataks in Perlebandet in order to reexamine metamorphic fluid composition, considering possibility of coexistence with CO_2-bearing fluid.

The studied sample is a garnet-sillimanite-biotite gneiss whose gneissose structure is cut by ~ 1 mm-thick black selvage. The selvage is mainly composed of Cl-rich biotite (~ 0.7 wt% Cl). Andalusite is exclusively present within the selvage. This suggests that Cl-bearing aqueous fluid infiltrated through a thin crack under andalusite stability field during retrograde metamorphism. In the wall rock, garnet breakdown to biotite + cordierite intergrowth is observed. Within the intergrowth, biotite has ~ 0.2-0.3 wt% Cl. In addition, CO_2 and H_2O peaks were detected in cordierite by Raman spectroscopy. This suggests that the Cl- and CO_2-bearing aqueous fluid triggered the garnet breakdown reaction. The *P-T* conditions of garnet breakdown were estimated to be ~750 ºC and ~ 0.3 GPa (cf. Spear et al., 1999). Since the selvage cuts the garnet breakdown texture, garnet breakdown reaction is followed by the selvage-forming fluid infiltration. Using the equation of Kaindl et al. (2006), CO_2 concentration in cordierite was estimated to be ~1.3-1.7 wt%. Chlorine concentration of fluid coexisting with biotite within the intergrowth texture was calculated to be ~ 30 wt% Cl and ~ 12 wt% Cl respectively in the case of melt-present and melt-absent conditions (Chevychelov et al., 2008; Aranovich, 2017). These values are considered to be upper limits for NaCl concentration in the fluid. The NaCl-CO_2-H_2O diagram indicates that the NaCl- and CO_2-bearing aqueous fluid is present as a single phase at ~ 750 ºC and ~ 0.3 GPa (Shmulovich and Graham, 2004). In addition, the re-integrated composition of the matrix perthite gave the equilibrium temperature of 800-900 ºC, assuming pressure condition to be 0.8-1.0 GPa (cf. Kawakami et al., 2017), using solvus of Fuhrman and Lindsley (1988), Kroll et al. (1993) and Benisek et al. (2004). Garnet-biotite gneiss from the same outcrop has nanogranitoids, which are direct evidence for patrial melting, as inclusions in garnet porphyroblast and monazite.

These observations suggest multiple post-peak fluid infiltration and decompression-cooling path in southern Perlebandet; peak metamorphism with partial melts followed by garnet breakdown reaction triggered by Cl- and CO_2-bearing aqueous fluid infiltration and Cl-bearing aqueous fluid infiltration under andalusite stability field. This study does not show counter-clockwise *P-T* path. This is probably due to the granitic body beneath the metamorphic rocks. Therefore, relationship between the metamorphic history constrained from the northern part of Perlebandet and this study should be further examined.

References

Aranovich, L. Y. (2017). The role of brines in high-temperature metamorphism and granitization. Petrology, 25(5), 486-497.

Asami, M., Suzuki, K., Grew, E. S. (2005). Monazite and zircon dating by the chemical Th-U-total Pb isochron method (CHIME) from Alasheyev Bight to the Sør Rondane Mountains, East Antarctica: a reconnaissance study of the Mozambique Suture in eastern Queen Maud Land. The Journal of geology, 113(1), 59-82.

Benisek, A., Kroll, H., Cemic, L. (2004). New developments in two-feldspar thermometry. American Mineralogist, 89(10), 1496-1504.

Chevychelov, V. Y., Botcharnikov, R. E., Holtz, F. (2008). Experimental study of fluorine and chlorine contents in mica (biotite) and their partitioning between mica, phonolite melt, and fluid. Geochemistry International, 46(11), 1081-1089.

Fuhrman, M. L., Lindsley, D. H. (1988). Ternary-feldspar modeling and thermometry. American mineralogist, 73(3-4), 201-215.

Higashino, F., Kawakami, T., M. Satish-Kumar, Ishikawa, M., Maki, K., Tsuchiya, N., Grantham, G.H., Hirata, T. (2013). Chlorine-rich fluid or melt activity during granulite facies metamorphism in the Late Proterozoic to Cambrian continental collision zone- An example from the Sør Rondane Mountains, East Antarctica. Precambrian Research 234, 229-246.

Higashino, F., Kawakami, T., Tsuchiya, N., Satish-Kumar, M., Ishikawa, M., Grantham, G., Sakata, S., Hirata, T. (2019). Brine infiltration in the middle to lower crust in a collision zone: mass transfer and microtexture development through wet grain–boundary diffusion. Journal of Petrology, 60(2), 329-358.

Jacobs, J., Bauer, W., Fanning, C.M. (2003). Late Neoproterozoic/Early Paleozoic events in central Doronning Maud Land and significance for the southern extension of the East African Orogen into East Antarctica. Precambrian Research 126, 27-53.

Kaindl, R., Tropper, P., Deibl, I. (2006). A semi-quantitative technique for determination of CO_2 in cordierite by Raman spectroscopy in thin sections. European Journal of Mineralogy, 18(3), 331-335.

Kawakami, T., Higashino, F., Skrzypek, E., Satish-Kumar, M., Grantham, G., Tsuchiya, N., Ishikawa, M., Sakata, S., Hirata, T. (2017). Prograde infiltration of Cl-rich fluid into the granulitic continental crust from a collision zone in East Antarctica (Perlebandet, Sør Rondane Mountains). Lithos 274-275, 73-92.

Kroll, H., Evangelakakis, C., Voll, G. (1993). Two-feldspar geothermometry: a review and revision for slowly cooled rocks. Contributions to Mineralogy and petrology, 114(4), 510-518.

Liebscher, A., Heinrich, C. A. (2007). Fluid–fluid interactions in the Earth's lithosphere. Reviews in Mineralogy and Geochemistry, 65(1), 1-13.

Meert, J. (2003). A synopsis of events related to the assembly of eastern Gondwana. Tectonophysics 362, 1-40.

Mieth, M., Jacobs, J., Ruppel, A., Damaske, D., Läufer, A., & Jokat, W. (2014). New detailed aeromagnetic and geological data of eastern Dronning Maud Land: Implications for refining the tectonic and structural framework of Sør Rondane, East Antarctica. Precambrian Research, 245, 174-185.

Osanai, Y., Nogi, Y., Baba, S., Nakano, N., Adachi, T., Hokada, T., Toyoshima, T., Owada, M., Satish-Kumar, M., Kamei, A., Kitano, I. (2013). Geologic evolution of the Sør Rondane Mountains, East Antarctica: Collision tectonics proposed based on metamorphic processes and magnetic anomalies. Precambrian Research 234, 8-29.

Shiraishi, K., Osanai, Y., Ishizuka, H., Asami, M. (1997) Geological map of the Sør Rondane Mountains, Antarctica. Antarctic Geological Map Series, Sheet 35, scale 1 : 250 000. National Institute of Polar Research, Tokyo.

Shiraishi, K., Dunkley, D. J., Hokada, T., Fanning, C. M., Kagami, H., Hamamoto, T. (2008). Geochronological constraints on the Late Proterozoic to Cambrian crustal evolution of eastern Dronning Maud Land, East Antarctica: a synthesis of SHRIMP U-Pb age and Nd model age data. Geological Society, London, Special Publications 308, 21-67.

Shmulovich, K. I., Graham, C. M. (2004). An experimental study of phase equilibria in the systems H_2O–CO_2–$CaCl_2$ and H_2O–CO_2–NaCl at high pressures and temperatures (500–800 ºC, 0.5–0.9 GPa): geological and geophysical applications. Contributions to Mineralogy and Petrology, 146(4), 450-462.

Spear, F. S., Kohn, M. J., Cheney, J. T. (1999). P-T paths from anatectic pelites. Contributions to mineralogy and petrology, 134(1), 17-32.

Uno, M., Okamoto, A., Tsuchiya, N. (2017). Excess water generation during reaction-inducing intrusion of granitic melts into ultramafic rocks at crustal P–T conditions in the Sør Rondane Mountains of East Antarctica. Lithos, 284, 625-641.

Sulfide mineralogy and whole-rock sulfur isotope composition of high-grade metamorphic rocks from the Sør Rondane Mountains, East Antarctica

Tetsuo Kawakami[1], Satish-Kumar, M.[2], Tokuya Mitsubori[2] and Sasidharan Silpa Ammini[2,3]
[1]*Kyoto University*
[2]*Niigata University*, [3]*Shimane University*

The lower crustal rocks of the ca. 650-500 Ma continental collision zone are widely exposed in the Sør Rondane Mountains, East Antarctica. Bounded by the Main Tectonic Boundary (MTB), which is considered to be the collision boundary, granulite facies rocks are mainly distributed in the NE terrane and rocks below amphibolite facies to granulite facies grade are distributed in the SW terrane (Osanai et al., 2013). Recently, ultrahigh-temperature (UHT) metamorphic rock is newly found from the Balchenfjella area in the NE terrane (Higashino & Kawakami, 2022).

Among these metamorphic rocks, sulfide-rich lithologies are found mainly in the Brattnipene and Balchenfjella areas. The sulfides are mostly phyrrotite and pyrite, which often occur in an irregular form at grain boundaries in the rock matrix. In some samples, a small number of sulfides are also found as inclusions in garnet and clinopyroxene. In this study, we measured the whole-rock sulfur isotopic compositions (^{32}S, ^{33}S, ^{34}S, and ^{36}S) of samples containing the sulfides. Bulk rock powders were used to extract sulfur (see Banerjee et al., 2021 for further details on measurement procedures) and results likely reflect the sulfur isotopic composition of the sulfide minerals in the matrix. There is no record of sulfur with mass-independent isotope fractionation, hawever the felsic gneisses, such as garnet-biotite gneiss and garnet-sillimanite gneiss, gave a wide range of $\delta^{34}S_{(CDT)}$ values from -7.0 to +12.0 ‰. These values overlap with sulfur isotopic composition of modern sedimentary sulfides and granitoid rocks (Giacometti et al., 2014). On the other hand, the values for mafic gneisses such as garnet-orthopyroxene-biotite gneiss and garnet-hornblende gneiss ranged from -6.0 to +3.9 ‰, which is consistent with the values previously reported from basalts and gabbros, except for one sample. The mafic gneiss sample that gave a $\delta^{34}S$ value (+12.8 ‰) largely different from published basalt and gabbro values is the one from the Brattnipene area. This sample is a wall rock part of the garnet-orthopyroxene-hornblende gneiss that is discordantly cut by the garnet-hornblende selvage. Higashino et al. (2015, 2019a) found a diffusion profile of chlorine concentration around a garnet-hornblende selvage, which they interpreted to be the trace of saline fluid infiltration during the retrograde metamorphism. Detailed petrological study have shown that the wall rock around the selvage was also affected by saline fluid infiltration (Higashino et al., 2019a), so the sulfur isotopic compositions obtained in this study are likely traces of sulfur-bearing saline fluid infiltration that was involved in the formation of the garnet-hornblende selvage. The high $\delta^{34}S$ value (+12.8 ‰) is close to that indicated by sulfate in seawater or sedimentary sulfides and granitic rocks (e.g., Giacometti et al., 2014). Hornblende and biotite selgaves similar to the garnet-hornblende selvage that cut gneissose structures are widely distributed throughout the Sør Rondane Mountains, suggesting that saline fluid infiltration occurred during the retrograde metamorphism in the entire Sør Rondane Mountains. The results of this study indicate that these retrograde metamorphic saline fluids may be seawater or fluids released during the crystallization of granitoids or partial melts. In fact, in the matrix of felsic gneisses of the Brattnipene, for which high $\delta^{34}S$ values (+9.1 ‰) were obtained in this study, we observed microstructures in which garnet is replaced by mineral intergrowth containing sulfides + cordierite due to fluid influx during the retrograde metamorphism (Ikeda et al., 2021). Therefore, not only mafic gneisses but also some felsic gneisses with high $\delta^{34}S$ values may have been affected by the infiltration of saline fluids during the retrograde metamorphism, similar to the fluids involved in the formation of the garnet-hornblende selvage. Higashino et al. (2019b) studied the oxygen isotopic zoning of felsic gneisses from Barchenfjella and found that $\delta^{18}O$ is significantly lower in the garnet rim. Based on this, they infer that the fluid responsible for the formation of the chlorine-rich biotite included in the garnet rim has a low $\delta^{18}O_{(V\text{-}SMOW)}$ value, and therefore, the origin of the fluid is inferred to be mafic rocks. The $\delta^{34}S$ value of this sample was determined as +5.4 ‰ in this study. Therefore, as in the case of hornblende and biotite selvages that cut the gneissose structure, we can also consider the involvement of sulfur-containing fluids of seawater origin.

In summary, while the origin of fluids involved in the formation of chlorine-rich minerals from the Sør Rondane Mountains may vary by metamorphic stage, they may also be understood in a unified manner as an influx of sulfur-bearing fluids of seawater origin. Further evaluation of more samples with multiple isotopic systems is needed in the future studies.

References

Banerjee, A. Satish-Kumar, M. & Chakrabarti, R., Sulfur, carbon and oxygen isotopic compositions of Newania carbonatites of India: implications for the mantle source characteristics. Journal of Mineralogical and Petrological Science, 116, 121-128, https://doi.org/10.2465/jmps.201130e , 2021

Giacometti, F., Evans, K. A., Rebay, G., Cliff, J., Tomkins, A. G., Rossetti, P., Vaggelli, G., & Adams, D. T., Sulfur isotope evolution in sulfide ores from Western Alps: Assessing the influence of subduction-related metamorphism, Geochem. Geophys. Geosyst., 15, 3808– 3829, doi:10.1002/2014GC005459, 2014

Higashino, F., & Kawakami, T., Ultrahigh-temperature metamorphism and melt inclusions from the Sør Rondane Mountains, East Antarctica. Journal of Mineralogical and Petrological Science, 117, https://doi.org/10.2465/jmps.220325, 2022

Higashino, F., Kawakami, T., Tsuchiya, N., Satish-Kumar, M., Ishikawa, M., Grantham, G. H., Sakata, S., Hattori, K., & Hirata, T., Geochemical behavior of zirconium during Cl-rich fluid or melt infiltration under upper amphibolite facies metamorphism - A case study from Brattnipene, Sør Rondane Mountains, East Antarctica. Journal of Mineralogical and Petrological Sciences, 110(4). https://doi.org/10.2465/jmps.150220, 2015

Higashino, F., Kawakami, T., Tsuchiya, N., Satish-Kumar, M., Ishikawa, M., Grantham, G., Sakata, S., & Hirata, T., Brine Infiltration in the Middle to Lower Crust in a Collision Zone: Mass Transfer and Microtexture Development Through Wet Grain-Boundary Diffusion. Journal of Petrology, 60(2), 329–358. https://doi.org/10.1093/petrology/egy116, 2019a

Higashino, F., Rubatto, D., Kawakami, T., Bouvier, A.-S., & Baumgartner, L. P. Oxygen isotope speedometry in granulite facies garnet recording fluid/melt–rock interaction (Sør Rondane Mountains, East Antarctica). Journal of Metamorphic Geology, 37(7). https://doi.org/10.1111/jmg.12490, 2019b

Ikeda, H., Kawakami, T., & Higashino, F. 2021, Counterclockwise and clockwise P-T histories recorded in a single sample? (Brattnipene, Sør Rondane Mountains, East Antarctica). The 12th Symposium on Polar Science, 2021.11.15-18.

Osanai, Y., Nogi, Y., Baba, S., Nakano, N., Adachi, T., Hokada, T., Toyoshima, T., Owada, M., Satish-Kumar, M., Kamei, A., & Kitano, I., Geologic evolution of the Sør Rondane Mountains, East Antarctica: Collision tectonics proposed based on metamorphic processes and magnetic anomalies. Precambrian Research, 234, 8–29. https://doi.org/10.1016/j.precamres.2013.05.017, 2013

Infiltration of K-Cl-rich fluid in mafic granulite from Austhovde

Y. Hiroi[1, 2], T. Hokada[2], T. Adachi[3], A. Kamei[4], K. Shiraishi[2], and Y. Motoyoshi[2]

[1]*Chiba University*

[2]*Ntional Institute of Polar Research*

[3]*Kyushu University*

[4]*Shimane University*

Mafic granulite sample 84012223 from Austhavde, Lützo-Holm Complex in East Antarctica, is a heterogeneous rock ranging from eclogitic part to amphibolitic part. The eclogitic part is composed maily of clinopyroxene and garnet, the latter enclosing numerous inclusions including various felsite-nanogranite inclusions (FNIs). The eclogitic part is poor in K and a small amount of biotite occurs only as inclusions in garnet, although a trace amount of k-feldspar is present as lamellae in plagioclase and a constituent of FNIs in garnet. The amphibolitic part consists mainly of hornblende with lesser amounts of plagioclase, orthopyroxene, biotite and quartz. It is poor in Si and rich in K, Ba, Pb, Rb, and Sr (Table 1). Biotite shows a local concentration along a plane (Fig. 1), suggesting that K- and Cl-rich fluid infiltrated along a fracture. Hornblende in the biotite-rich part is heterogeneous; the outer part is locally enriched in K and Cl (Figs. 1 & 2 and Table 2). In addition, both hornblende and orthopyroxene in the biotite-rich part are more Fe-rich compared to those far from the biotite-rich part even in the same amphibolitic part. Plagioclase also shows various compositions (An_{38-80}) from garin to grain in the biotite-rich part (Fig. 1).

The distinct differences in the mode of occurrence and chemical compositions of minerals, especially biotite and hornblende, between eclogitic and amphibolitic parts indicate that FNIs in garnet in elcogitic part are not the products of K- and Cl-rich fluid infiltration, which introduced LILE into the rock. Similar fluid activity after the peak of granulite-facies regional metamorphism has been well documented in the Sør Rondane Mountains in East Antarctica (e.g. Higashino et al., 2019).

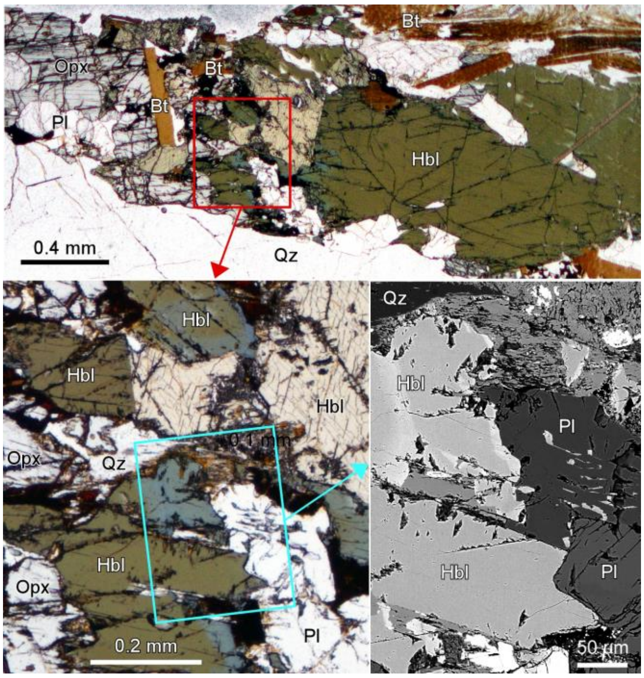

Figure 1. Biotite-rich part of amphibolitic part of mafic granulite sample 84012223 from Austhovde. Note heterogeneous hornblende.

Table 1. Bulk rock composition of amphibolitic part of mafic granulite sample 84012223

SiO_2	40.82	Ba	800
TiO_2	2.23	Ce	54
Al_2O_3	14.52	Cr	86
$Fe_2O_3^{\dagger}$	21.80	Ga	5
MnO	0.34	Nb	25
MgO	6.46	Ni	63
CaO	9.99	Pb	24
Na_2O	1.35	Rb	32
K_2O	1.99	Sr	226
P_2O_5	0.17	Th	17
H_2O	0.25	V	637
Total	99.92	Y	59
$X_{Mg}^{\#}$	0.370	Zr	106

Mole MgO/(MgO + total Fe as FeO)

Table 2. K-Cl-rich hornblende in biotite-rich part

SiO_2	36.24
TiO_2	0.62
Al_2O_3	14.72
Cr_2O_3	0.08
FeO	24.19
MnO	0.14
MgO	4.23
CaO	11.49
Na_2O	1.19
K_2O	2.63
F	0.05
Cl	3.68
-O	0.85
total	98.41

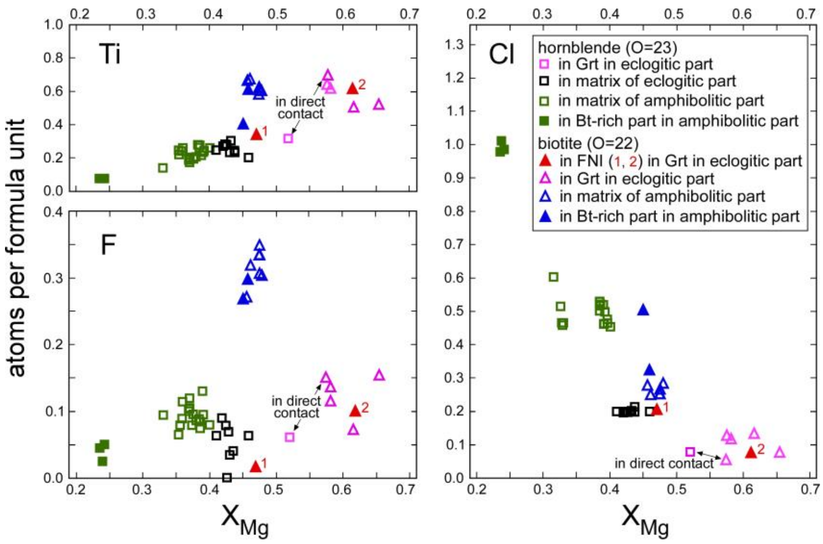

Figure 2. Compositions of hornblende and biotite in mafic granulite sample 84012223 from Austhovde.

Reference

Higashino et al., Brine infiltration in the middle to lower crust in a collision zone: Mass transfer and microtexture development through wet grain-boundary diffusion. Journal of Petrology, 60, 329-358, 2019.

Series of fluid activities during brittle-viscous shear deformation in amphibolite on the southern side of the Main Shear Zone, Ketelersbreen, Sør Rondane Mountains, East Antarctica

Mindaleva Diana[1], Masaoki Uno[1], Fumiko Higashino[2], Tatsuro Adachi[3], Tetsuo Kawakami[2] and Noriyoshi Tsuchiya[1]
[1]*GSES, Tohoku University*
[2]*Department of Geology and Mineralogy, Graduate School of Science, Kyoto University*
[3] *Faculty of Social and Cultural Studies, Kyushu University*

Fluid flow in the crust causes hydration reactions, which induce mass transport, change the rheology of rocks, and plays a crucial role in triggering earthquakes, tremors, and slow slip events. Recent geophysical findings of slow earthquakes revealed that source regions of slow earthquakes locate brittle-viscous transition zones, and are high in fluid pressure (Behr and Burgmann, 2021). Geological observation of fluid-induced shear fracturing at brittle-viscous transition zones would provide important constraints on the physico-chemical processes in the source region of slow earthquakes. This study provides a primary analysis of series of fluid activities in amphibolite samples collected nearby the Main Shear Zone (MSZ) exposed along the Ketelersbreen, Sør Rondane Mountains (SRM), East Antarctica, and reveal their temperature conditions of fluid infiltration related to brittle-viscous shear deformation.

A series of amphibolite samples were collected from the southern side of the MSZ exposed along the Ketelersbreen, Sør Rondane Mountains, East Antarctica (S 72.103°, E 23.199°) during the 61st Japan Antarctic Research Expedition in 2019-2020. The MSZ is one of the major shear zones in the eastern Dronning Maud Land, lasting approximately 120 km, with a width of several hundred meters. MSZ is characterized by dextral high-strain ductile deformation under peak amphibolite-facies conditions (Ruppel et al., 2015). MSZ at the SRM was first defined by Kojima and Shiraishi (1986) and represented the boundary between northern amphibolite-facies metamorphic rocks and southern older meta-tonalite.

The amphibolite is associated with foliation parallel quartz veins (Fig. 1a), are cut by light-coloured muscovite-calcite-amphibole (Ms-Cc-Amp) bearing veins (Fig. 1b, c). Epidote alteration layers occur along high-angle dark-coloured amphibole veins and/or along foliation, and cut all the structure mentioned above (Fig. 1d, e).

Amphibolite host rock mainly consists of tschermakite, plagioclase, quartz, sphene and relict clinopyroxene. The relict clinopyroxene (X_{Mg} = 0.75) is found as inclusion in the quartz grains. Ms-Cc-Amp-bearing veins contain muscovite, calcite, amphibole, plagioclase, quartz, zoisite, and apatite. Along the Ms-Cc-Amp-bearing veins, mm-sized echelon veins occur in the amphibolite (Fig. 1e), and consist of tschermakite, chlorite, plagioclase, quartz, magnetite, and apatite. The dark-coloured amphibole veins contain actinolite, hornblende, calcite, epidote, quartz, apatite, and relict clinopyroxene. In the dark-coloured amphibole veins, an actinolite rim surrounds the hornblende core. Epidote alteration layer consist of epidote, calcite, sphene, plagioclase, actinolite, quartz, and apatite.

We observe shear displacement along the Ms-Cc-Amp-bearing vein (Fig. 1b). On the other hand, the host rocks and echelon veins are deformed along the Ms-Cc-Amp-bearing veins, and record brittle-viscous shear deformation (Fig. 1c).

The range of X_{Ab} in plagioclase in the amphibolite host rock is 0.60-0.64, while that in the echelon vein is 0.54-0.62. The Si contents in amphiboles are 6.7-6.8 atoms per formula unit (a.p.f.u., O=23), and Na contents are 0.4 a.p.f.u. Hornblende plagioclase thermobarometer (Holland and Blundy, 1994) was used to estimate temperature conditions of host rock metamorphism. Temperature conditions estimated for the amphibolite host rock are 595±65 °C in the range of 0-1.5 GPa.

We analysed Cl content in amphibole in the Ms-Cc-Amp veins and the host rock. The highest Cl concentration was detected in the vein centre (0.62 wt%), and the lowest one was in the host rock (0.01 wt%).

Several fluid activities are suggested from the presence of different veins with different types of amphiboles and alteration layers. At the first stage of hydration, clinopyroxene in the host rock is likely to have broken down to tschermakite. As the host rock lacks carbonate nor carbonaceous materials, infiltration of CO_2-bearing fluids along foliation and veins are required to form calcite. Secondly, Cl and CO_2-bearing fluids infiltrated to form Ms-Cc-Amp veins, accompanying brittle-viscous shear deformation. Thirdly, CO_2-bearing fluids infiltrated along fractures and foliation, to form high-angle amphibole veins and epidote alteration, that contains actinolite formed at low-temperature consistent with later stage of fluid infiltration. These series of fluid activities had occurred during the brittle-viscous transitions and the cooling of the southern part of the Main Shear Zone, and would provide physico-chemical insights for fluid-induced rock fracturing during brittle-viscous transitions in the crust.

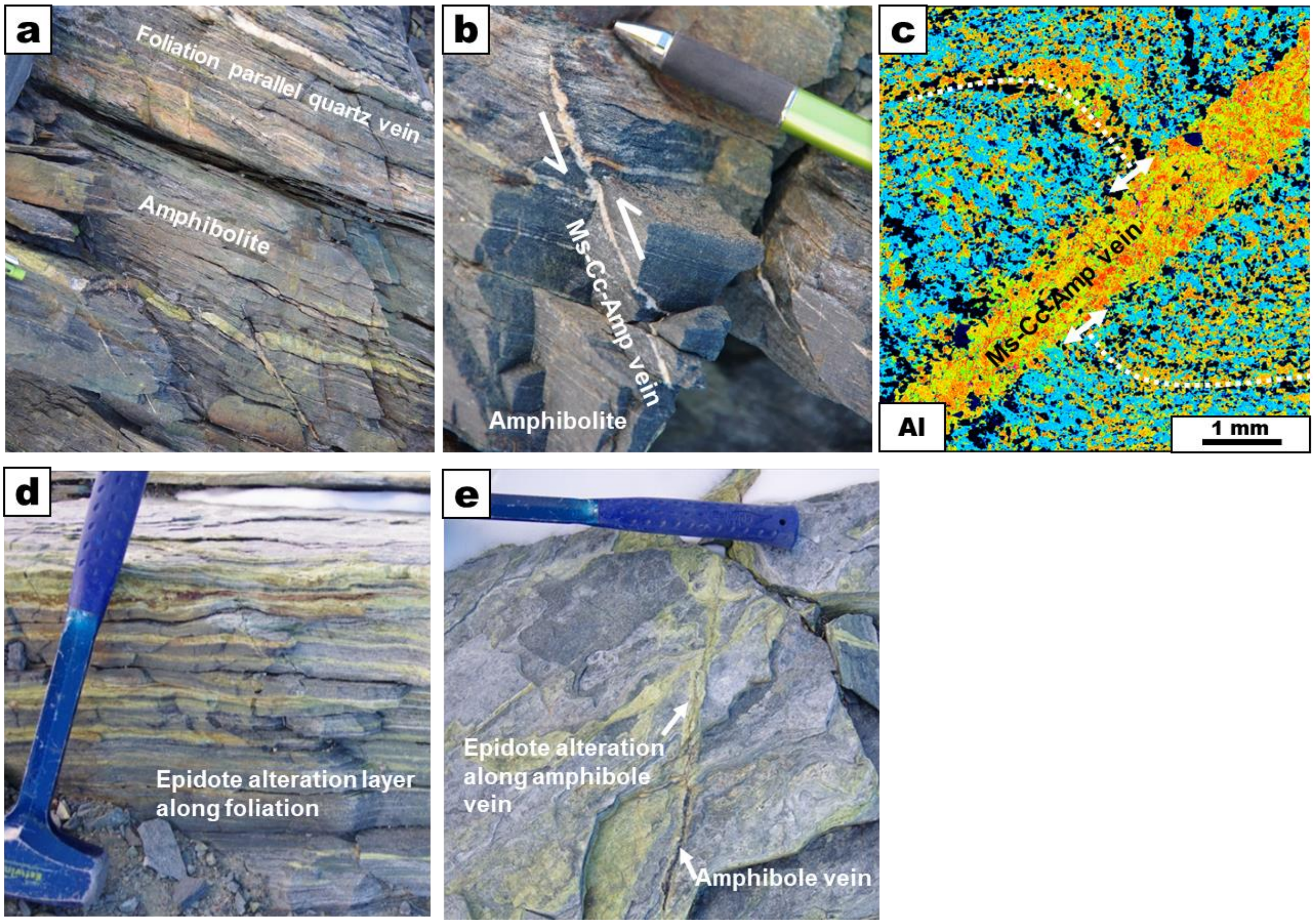

Figure 1. (a) Outcrop photographs of amphibolite containing foliation parallel quartz veins. (b) Light-colored muscovite-calcite-amphibole bearing veins. The white arrow showing the direction of the shear. (c) X-ray elemental map of Al showing viscous shear displacement along a muscovite-calcite-amphibole bearing vein. Echelon veins are shown by white dotted lines. (d) Epidote alteration layer along foliation in amphibolite. (e) Epidote alteration along high-angle dark-coloured amphibole veins.

References

Behr, Whitney M., and Roland Bürgmann. What's down there? The structures, materials and environment of deep-seated slow slip and tremor. Philosophical Transactions of the Royal Society A 379.2193, 2021.

Holland, T., and Blundy, J, Non-ideal interactions in calcic amphiboles and their bearing on amphibole-plagioclase thermometry, Contributions to mineralogy and petrology, 116(4), 433-447, 1994.

Ruppel, Antonia S., et al., The Main Shear Zone in Sør Rondane, East Antarctica: Implications for the late-Pan-African tectonic evolution of Dronning Maud Land, Tectonics 34.6: 1290-1305, 2015.

Kojima, Satoru, and Kazuyuki Shiraishi, Note on the geology of the western part of the Sør Rondane Mountains, East Antarctica,: 116-131, 1986.

Metamorphic condition and age of a pelitic gneiss from Niban-nishi Rock of Niban Rock in the Lützow-Holm Complex, East Antarctica

Yuki Mori[1,2], Tomokazu Hokada[3,4] , Tomoharu Miyamoto[1], and Takeshi Ikeda[1]
[1]*Kyushu University*
[2]*Japan Synchrotron Radiation Research Institute (JASRI/SPring-8)*
[3]*National Institute of Polar Research*
[4]*The Graduate University for Advanced Studies (SOKENDAI)*

The Lützow-Holm Complex (LHC) in eastern Dronning Maud Land, East Antarctica is a Neoproterozoic-Cambrian high-grade metamorphic complex extending for about 500 km along Prince Olav Coast and Soya Coast. The LHC has been characterized by continuous increase in metamorphic grade from northeast to southwest (Hiroi et al., 1991) and metamorphic age of 600–520 Ma (Dunkley et al., 2020 and reference therein). The LHC is divided into three metamorphic zones referred to as the amphibolite-facies zone, transitional zone, and granulite-facies zone from northeast to southwest (Hiroi et al., 1991). Cape Hinode located in the amphibolite-facies zone is known as that the exposure shows different features from other exposures in the LHC such as Tonian metamorphic age of 1017–960 Ma, granulite-facies metamorphic rocks, and tonalite dominant lithology (Yanai and Ishikawa, 1978; Shiraishi et al., 1994; Hiroi et al., 2006, 2008; Dunkley et al., 2014). Recently, Baba et al. (2021) revealed that Akebono Rock, an exposure located about 12 km northeast of Cape Hinode in the amphibolite-facies zone, records Tonian metamorphism of 977–917 Ma. Baba et al. (2021) reported that garnet preserves prograde zoning and kyanite is stable in the matrix in Akebono Rock. Niban rock is a 2.5 km x 3.5 km exposure located in amphibolite-facies zone of the LHC and located at about 15 km to the southwest of Cape Hinode. Niban Rock is underlain mainly by sillimanite-garnet-biotite gneiss, biotite gneiss, and biotite-hornblende gneiss with minor metabasite, calc-silicate gneiss, granite, and aplite (Kizaki et al., 1983). In Niban Rock, Dunkley et al. (2014) conducted zircon U–Pb dating and monazite U–Th–Pb dating and reported 551 Ma as magmatic age and 532 Ma as metamorphic age from metagranitic dyke and 940 Ma as protolith age from augen granitic orthogneiss. Kitano et al. (2021) reported zircon U–Pb age of 998 Ma as metamorphic age from Niban Rock. However, comprehensive analysis of metamorphism including detailed textural observation, mineral chemistry, whole-rock chemistry, P–T condition, and age was not performed at Niban Rock yet. In this study, we describe a garnet-bearing migmatitic pelitic gneiss collected from Niban-nishi Rock of Niban Rock in the LHC. We estimated the P–T condition of retrograde stage based on garnet–biotite geothermometer and garnet–sillimanite–quartz–plagioclase geobarometer. Phase equilibrium modeling was applied to determine the minimum temperature required for partial melting and constrain peak metamorphic temperature. Monazite electron microprobe U–Th–Pb dating was also performed, and we revealed that the gneiss was suffered from Tonian metamorphism.

The studied pelitic gneiss (sample no. TM11020804A) was collected from Niban-nishi Rock in Niban Rock during the 52nd Japanese Antarctic Research Expedition (JARE 52). The gneiss is composed mainly of quartz, plagioclase, biotite, sillimanite, K-feldspar, muscovite, garnet with minor amounts of zircon, monazite, apatite, and ilmenite. The gneiss shows foliation defined by shape-preferred orientations of sillimanite, biotite, muscovite, and quartz. Monazite occurs in the matrix and as inclusion in biotite or garnet (up to 0.1 mm long). Compositional zoning in garnet shows outward decrease in Xalm and increase in Xsps, which is regarded as retrograde zoning. Garnet–biotite geothermometer of Holdaway (2000) and garnet–sillimanite–quartz–plagioclase geobarometer of Holdaway (2001) were used for the estimation of retrograde condition. We used the compositions of rims of matrix garnet, biotite, and plagioclase and obtained 620–670 °C and 0.42–0.60 GPa as the retrograde condition of regional metamorphism. We also performed phase equilibrium modeling based on the result of whole-rock chemical analysis using a free energy minimization software Perple_X (Connolly, 2005, 2009) to obtain stable mineral assemblages in each P–T condition. Based on detailed textural observation, we consider that the most plausible mineral assemblage at peak metamorphism was garnet + biotite + melt + ilmenite + plagioclase + K-feldspar + sillimanite + quartz. According to the P–T pseudosection, the assemblage is stable under 690–830 °C and 0.35–0.80 GPa, and thus we consider that the peak metamorphic temperature was lower than ~830 °C. Monazite electron microprobe U–Th–Pb dating has an advantage that we can clarify the occurrence of analyzed monazite. As a result, we obtained the weighted mean age of 940.1 ± 9.8 Ma (MSWD = 0.31, 2σ level) from the 62 ages of 1015–889 Ma. We regarded that there is no relation between the occurrence of monazite and the obtained ages. Based on detailed textural observation, the age obtained in this study corresponds to the timing of metamorphism from prograde to retrograde stages. The metamorphic age is consistent with the neighboring exposures of Cape Hinode and Akebono Rock, but the metamorphic grade is lower than Cape Hinode and compositional zonation of garnet and stable phase of alminosilicate are different from Akebono Rock.

References

Baba, S., Horie, K., Hokada, T., Takehara, M., et al., Newly found Tonian metamorphism in Akebono Rock, eastern Dronning Maud Land, East Antarctica. Gondwana Research, 105, 243–261, 2021.

Connolly, J.A.D., Computation of phase equilibria by linear programming: a tool for geodynamic modeling and its application to subduction zone decarbonation. Earth and Planetary Science Letter, 236, 524–541, 2005.

Connolly, J. A. D., The geodynamic equation of state: What and how. Geochemistry, Geophysics, Geosystems, 10, Q10014, 2009.

Dunkley, D.J., Shiraishi, K., Motoyoshi, Y., Tsunogae, T., Miyamoto, T., Hiroi, Y. and Carson, C., Deconstructing the Lützow-Holm Complex with zircon geochronology. 7th International SHRIMP Workshop, Abstract, 2014.

Dunkley, D.J., Hokada, T., Shiraishi, K., Hiroi, Y., Nogi, Y. and Motoyoshi, Y., Geological subdivision of the Lützow–Holm Complex in East Antarctica: From the Neoarchean to the Neoproterozoic. Polar Science, 26, 100606, 2020.

Hiroi, Y., Shiraishi, K., Motoyoshi, Y., Late Proterozoic paired metamorphic complexes in East Antarctica, with special reference to the tectonic significance of ultramafic rocks. In Geological Evolution of Antarctica (Thomson, M.R.A, Crame, J.A. and Thomson, J.W. Eds.), Cambridge University Press, Cambridge, 83-87, 1991.

Hiroi, Y., Motoyoshi, Y., Satish-Kumar, M., Kagashima, S., Suda, Y., Ishikawa, N., Granulites from Cape Hinode in the amphibolite-facies eastern part of Prince Olav Coast, East Antarctica: New evidence for allochthonous block in the Lützow-Holm Complex. Polar Geoscience, 19, 89-108, 2006.

Hiroi, Y., Motoyoshi, Y., Ishikawa, N., Hokada, T. and Shiraishi, K., Origin of xenocrystic garnet and kyanite in clinopyroxene–hornblende-bearing adakitic metatonalites from Cape Hinode, Prince Olav Coast, East Antarctica. In: Geodynamic Evolution of East Antarctica: A Key to the East–West Gondwana Connection (Satish–Kumar, M., Motoyoshi, Y., Osanai, Y., Hiroi, Y. and Shiraishi, K. Eds.), Geological Society of London, Special Publication, 333–350, 2008.

Holdaway, M.J., Application of new experimental and garnet Margules data to the garnet-biotite geothermometer. American Mineralogist, 85, 881-892, 2000.

Holdaway, M.J., Recalibration of the GASP geobarometer in light of recent garnet and plagioclase activity models and versions of the garnet–biotite geothermometer. American Mineralogist, 86, 1117-1129, 2001.

Kitano, I., Hokada, T., Baba, S., Kamei, A., et al., U–Pb zircon geochronology of high-grade metamorphic rocks from outcrops along the Prince Olav Coast, East Antarctica. The 12th Symposium on Polar Science Abstract, 2021.

Kizaki, K., Hiroi, Y., Kanisawa, S., Explanatory text of geological map of Niban Rock, Antarctica. Antarctic Geological Map Series, Sheet 17 Niban Rock. NIPR, Tokyo, 1983.

Shiraishi, K., Ellis, D.J., Hiroi, Y., Fanning, C.M., Motoyoshi, Y. and Nakai, Y., Cambrian orogenic belt in East Antarctica and Sri Lanka: implication for Gondwana assembly. Journal of Geology, 102, 47-65, 1994.

Yanai, K. and Ishikawa, T., Explanatory text of geological map of Cape Hinode, Antarctica. Antarctic Geological Map Series, Sheet 11 Cape Hinode. NIPR, Tokyo, 1978.

Zircon geochronology and geochemistry of syenites in the Yamato Mountains, East Antarctica

Kenji Horie[1, 2], Mami Takehara[1] and Tomokazu Hokada[1, 2]
[1]*National Institute of Polar Research*
[2]*The Graduate University for Advanced Studies, SOKENDAI*

The Yamato Mountains consist mainly of the granulite-facies and amphibolite-facies metamorphic rocks and intrusive syenitic rocks, and include seven massifs, called provisionally A, B, C, D, E, F and G from south to north, and associated nunataks. The syenite in the Yamato Mountains are not affected by deformation and recrystallization and then they are regarded as emplacing at the late stage of the regional metamorphism. Geochronological data for the Yamato Mountains are limited. Some K-Ar and Rb-Sr ages are reported for the syenites, granites, and metamorphic rocks (500-400 Ma, whole-rock; e.g., Yanai and Ueda, 1974, Kojima et al., 1982). Shibata et al. (1985, 1986) also obtained a Rb-Sr isochron age of 493.3 + 4.5 Ma (K-feldspar, plagioclase, biotite, and whole-rock), K-Ar ages of 480 Ma (biotite) and 502 Ma (hornblende) for the metamorphic rocks from the Yamato Mountains (Massif A). The zircon U-Pb dating of orthopyroxene biotite gneiss in Massif A shows high U overgrowth rims with 630-605 Ma (Shiraishi et al., 1994). Quartz monzonite of Massif A indicates the emplacement age of 532 ± 8 Ma (Shiraishi et al., 2003). Granitic gneiss of Massif B shows a weighted mean $^{206}Pb/^{238}U$ age of 539 ± 4 Ma with older cores of 630-570 Ma.

In this study, two syenites (73120307 and 92110701B) and biotite-pyroxene gneiss (92111401C) collected from Massif D were analyzed by a sensitive high-resolution ion microprobe (SHRIMP-IIe) at the National Institute of Polar Research, Japan. The weighted mean $^{206}Pb/^{238}U$ ages of 73120307 and 92110701B syenites are 537.9 ± 3.0 Ma (95% conf.) and 538.4 ± 3.0 Ma (95% conf.), respectively, which is consistent with the that of the quartz monzonite of Massif A. Chemical U-Pb dating of monazite in the 73120307 sample was carried out by an electron probe micro analyzer (JEOL JXA-8200) at National Institute of Polar Research. The monazite ages are scattered from 610 to 499 Ma and age peak center of a probability density is ca. 526 Ma. The zircon grains in the biotite-pyroxene gneiss show low response CL rim surrounding igneous (broad band to oscillatory) zoning core. The zircon cores suggest the igneous activity at 625.8 ± 4.3 Ma. The rim shows a weighted mean $^{206}Pb/^{238}U$ age of 548.5 ± 3.7 Ma, which indicates the timing of the regional metamorphism. Further information such as other trace element concentrations will be demonstrated.

References

Kojima, H., Nishida, T., and Yanai, K., Geology of the Belgica Mountains, Jap. Mem. Natl. Inst. Polar Res.; Spec. Issue 21, 32-64, 1982.

Shibata, K., Yanai, K., and Shiraishi, K., Rb-Sr mineral isochron ages of metamorphic rocks, East Antarctica, Jap. Mem. NatL Inst. Polar. Res.; Spec. Issue 37, 164-171, 1985.

Shibata, K., Yanai, K., and Shiraishi, K., Rb-Sr whole-rock ages of metamorphic rocks from eastern Queen Maud Land, East Antarctica, Jap. Mem. Natl. Inst. Polar. Res.; Spec. Issue 43, 133-148, 1986.

Shiraishi, K., Ellis, D. J., Hiroi, Y., Fanning, C. M., Motoyoshi, Y. and Nakai, Y., Cambrian orogenic belt in East Antarctica and Sri Lanka: implications for Gondwana assembly, The Journal of Geology, 102, 47-65, 1994.

Shiraishi, K., Hokada, T., Fanning, C.M., Misawa, K., and Motoyoshi, Y., Timing of thermal events in eastern Dronning Maud Land, east Antarctica, Polar Geosci., 16, 76-99, 2003.

Yanai, K., and Ueda, Y., Absolute ages and geological investigations on the rocks in the area around Syowa Station, East Antarctica, Nankyoku Shiryo (Antarct. Rec.) 48, 70-81 (in Japanese, with English abstract), 1974.

Multichronology of Harvey Nunatak, Napier Complex, East Antarctica

Mami Takehara[1], Kenji Horie[1,2] and Tomokazu Hokada[1,2]
[1] *National Institute of Polar Research, 10-3, Midori-cho, Tachikawa-shi, Tokyo 190-8518, Japan*
[2] *The Graduate University for Advanced Studies, SOKENDAI, 10-3, Midori-cho, Tachikawa-shi, Tokyo 190-8518, Japan*

Ultra-high temperature (UHT) metamorphism plays an essential role in developing and stabilizing continents through accretionary and collisional orogenesis. The Napier Complex in East Antarctica is where the regional UHT metamorphism was first recognized (Dallwitz,1968). This complex experienced extremely high temperatures (>1100 °C) based on the mineral assemblage of sapphirine + quartz (Harley, 2016 and reference therein). The thermal history of the Napier Complex is essential for unraveling the earth's crustal evolution, including deep crust; however, geochronological constraints, such as the timing and duration of the metamorphic events, are still debated.

Zircon, a valuable accessory mineral for geochronometers, has become a powerful geochemical tool for Antarctic geological and petrological research. We report preliminary U-Pb zircon ages of rock samples (sample Nos. 170223-2A-08 and 170223-2A-10) collected from Harvey Nunatak in the Napier Complex, East Antarctica, by JARE-58 Geological Field Survey Team. The rims of zircons in the cathodoluminescence images indicated weighted means of 2463 ± 10 Ma and 2452.8 ± 9.4 Ma (95% confidence, MSWD = 1.3 and 1.4, n = 14 and 13) analyzed using a sensitive high-resolution ion microprobe (SHRIMP-IIe) in NIPR.

We also found extremely lithium (Li)-enriched zircons (Li content, [Li]: ~300-600 ppm) in an orthopyroxene-felsic-gneiss (sample No. 170223-2A-09). The zircons were characterized according to the concentration of trace elements analyzed by SHRIMP-IIe in NIPR. The Li and oxygen isotope ratios of zircons are also analyzed by SHRIMP-IIe/AMC in NIPR. The Li isotope ratios (δ7Li) of the Li-rich zircons indicate a wide range from -2.8‰ to 12.7‰ (average is 3.5‰), which suggests the sources of the zircons were affected by contamination of sediment. The correlation between the Nb/Yb and U/Yb of zircons suggests a magmatic arc origin. Therefore, the protolith is derived from the magmatic arc, where sediments from the continental crust are subducted with water. In addition, some zircon grains have been affected by hydrothermal alteration recently since the zircons indicate high concentrations of non-formula elements and light REE. The altered domains indicate lower Li concentrations than those of unaltered domains.

In this presentation, we also report the U-Pb and trace element data in monazite and apatite in the same felsic gneiss (sample No. 170223-2A-09) and discuss based on the data.

References

Dallwitz (1968) Nature, 219, 476–477.
Harley (2016) J. Mineral. Petrol. Sci., 111, 50–72.

Dependence of GIA-induced gravity change in Antarctica on viscoelastic Earth structure

Yoshiya Irie[1], Jun'ichi Okuno[1,2], Takeshige Ishiwa[1,2], Koichiro Doi[1,2] and Yoichi Fukuda[1,3]
[1]*National Institute of Polar Research*
[2]*The Graduate University for Advanced Studies, SOKENDAI*
[3]*Kyoto University*

The Antarctic ice mass loss is accelerating due to recent global warming. Changes in Antarctic ice mass have been observed as the gravity change by GRACE (Gravity Recovery and Climate Experiment) satellites. The gravity signal includes both the component of the ice mass change and the component of the solid Earth response to surface mass change (Glacial Isostatic Adjustment, GIA). Therefore, estimates of the ice mass change from GRACE data require subtraction of GIA model predicted gravity rates (GIA correction).

Antarctica is characterized by lateral heterogeneity of seismic velocity structure. West Antarctica shows relatively low seismic velocities, suggesting low-viscosity regions in the upper mantle. On the other hand, East Antarctica shows relatively high seismic velocities, suggesting thick lithosphere. Here we examine the dependence of GIA correction on lithosphere thickness and upper mantle viscosity.

Figure 1 shows GIA correction based on the ice history model ICE-6G_D (Peltier *et al.*, 2018). The GIA correction for the average viscoelastic structure of West Antarctica (red diamond in Figure 1) is nearly identical to that for the average viscoelastic structure of East Antarctica (blue diamond in Figure 1). There is a trade-off between the lithosphere thickness and the upper mantle viscosity. This trade-off may reduce the effect of the lateral variations in viscoelastic Earth structure beneath Antarctica on the estimate of Antarctic ice mass change.

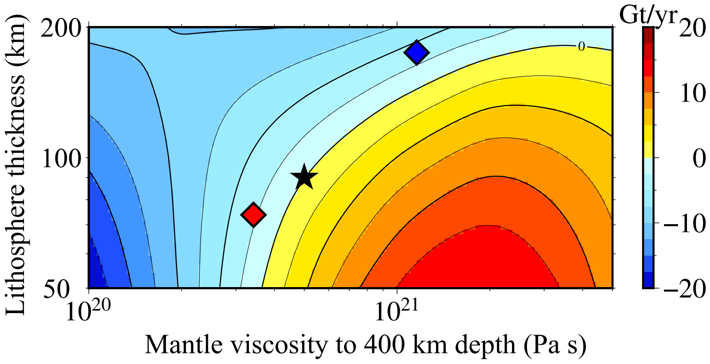

Figure 1. Predicted GIA corrections as a function of lithosphere thickness and mantle viscosity to 400 km depth using the ice history model ICE-6G_D (Peltier *et al.*, 2018). The values are plotted relative to the optimum viscoelastic Earth model of ICE-6G_D (black star), which is 90 Gt/yr. The warmer (colder) color indicates a larger (smaller) GIA correction than that for the optimum model. Red and blue diamonds are the averages of seismic-based viscoelastic Earth model $V3D_{RH}$ (Pan *et al.*, 2021) over West Antarctica and East Antarctica, respectively.

A study of the relationship between rapid flow velocity deceleration events of Shirase Glacier, East Antarctica, and the surrounding bathymetry

Shotaro Ohkawa[1], Koichiro Doi[1,2], Yuichi Aoyama[1,2]
[1]*Department of Polar Science, The Graduate University for Advanced Studies*
[2]*National Institute of Polar Research*

Introduction

Ice mass discharge by ice stream is one of the critical parameters in the mass balance estimation of the Antarctic ice sheet. To accurately estimate the depletion of the Antarctic ice sheet, it is essential to determine the cause of the flow rate fluctuations. Shirase Glacier, located in East Antarctica, is known to be one of the fastest-flowing glaciers in Antarctica. We estimated the glacier flow rate using images acquired by the Sentinel-1A synthetic aperture radar (SAR) and found that the glacier flow rate on the east side of Shirase Glacier was estimated to be 30-40 km downstream from the grounding line (GL) in 2020, and 55 km downstream from the GL in 2021. Different from seasonal fluctuations, a rapid decrease in flow velocity was found around 30-40 km downstream from the GL in 2020 and around the terminus 55 km downstream from the GL in 2021. In addition, we found that the slowdown of flow velocity propagated upstream. In order to clarify the cause of the rapid decrease in flow velocity, we compared the glacier thickness at the point where the rapid decrease occurred using ICESat-2 data with bathymetry data obtained from point echo sounding data via sea-ice drill holes.

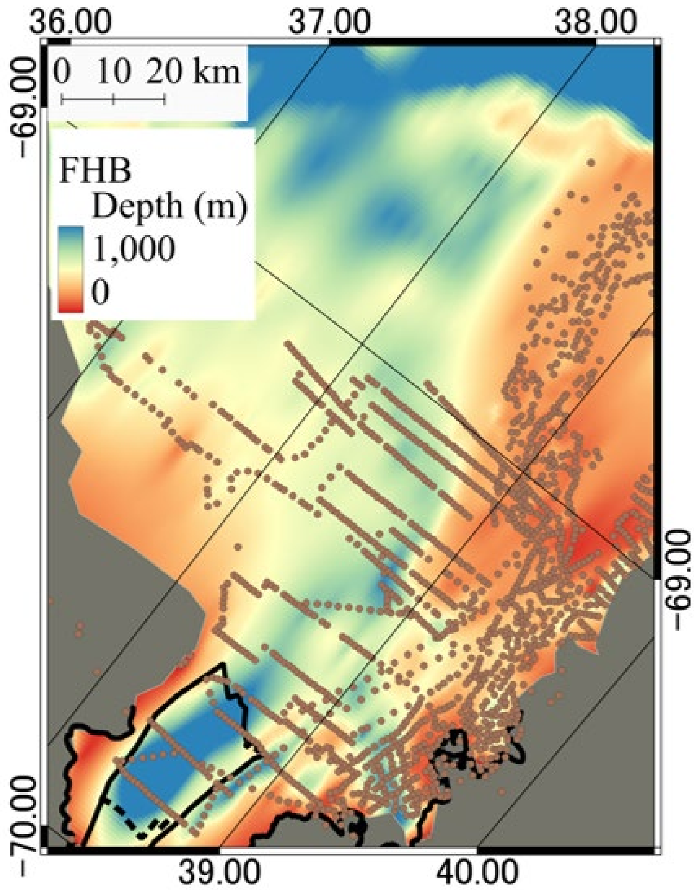

Figure 1. Bathymetric map of the Shirase Glacier area. The brown dots indicate the location of echo sounder observations on the ice (Hirano et al., 2020).

Data and Methods

To calculate glacier flow velocities in this study, offset tracking analysis was applied to SAR data of 103 scenes acquired by Sentinel-1A between July 26, 2018 and January 6, 2022. Surface elevation measured by ICESat-2 between 2018 and 2021 was used to measure surface elevation changes of the glacier and glacier-front icebergs; since the surface elevation obtained by ICESat-2 is the ellipsoid height the surface height above sea level can be approximated by subtracting the geoid height and the mean ocean dynamic from the ellipsoid height. Once the height above sea level is known, the thickness of glaciers and icebergs can be determined by assuming that the ice is floating. Assuming a glacier density of 900 kg m-3 and an ocean density of 1030 kg m-3, $H = 7.92\ h$, where H is the ice thickness and h is the height above sea level (e.g., Griggs and Bamber, 2011). The estimated ice thickness was compared to bathymetry data shown in Figure 1.

Results and Discussion

Figure 2 shows the flow velocity extracted every 10 km from GL. It is found that the glacier flows at an average rate of 70-80 m per cycle (= 12 days), with slower velocities around 30-40 km downstream from the GL from March to September 2020. Additionally, the flow velocity downstream of 55 km from the east side GL has been rapidly decreasing since April 2021. On the upstream side of the iceberg, the flow rate slows down after about 2-4 cycles.

Ice thickness was estimated from surface elevation data from ICESat-2 data and compared with bathymetry data for the glacier terminus and 30-40 km downstream from the GL, where the glacier flow rate had decreased rapidly (Figure 1). By taking the difference in surface elevation from the ice thickness and comparing it to the bathymetry, the relationship between the glacier and the bathymetry can be determined. This suggests that the icebergs ran aground in March 2020 and April 2021, causing the rapid slowdown. The slowdown of flow velocity in the upstream iceberg area is thought to have been caused by propagation of slowdown of the downstream icebergs to the upstream icebergs, such as when an upstream iceberg collides with a stranded iceberg, causing a slowdown, and then another upstream iceberg collides with those two icebergs.

Acknowledgments
This research was partially supported by Grant-in-Aid for Scientific Research (17H06321). We acknowledge and express our deep appreciation for the support.

References

Griggs and Bamber. (2011): Antarctic ice-shelf thickness from satellite radar altimetry, Journal of Glaciology, 57, 203, 485-498.

Hirano, D., Tamura, T., Kusahara, K. et al. Strong ice-ocean interaction beneath Shirase Glacier Tongue in East Antarctica. Nat Commun 11, 4221 (2020).

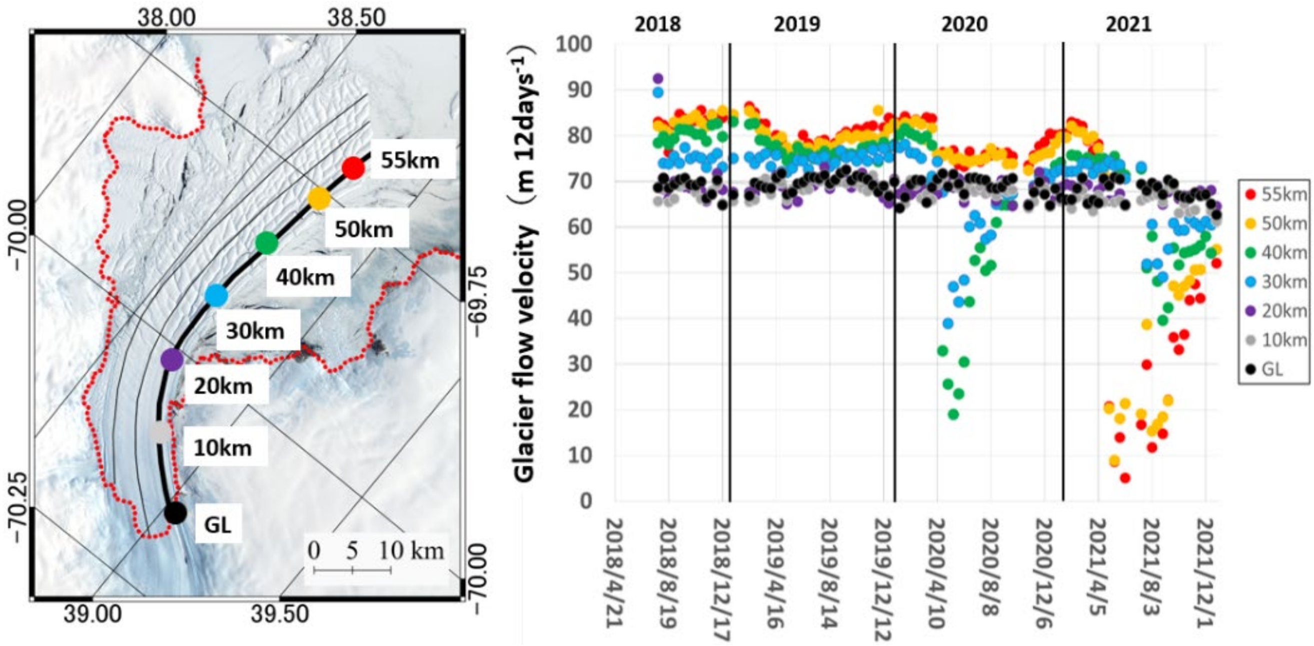

Figure 2. Flow speed of 10 km from GL on the east side of Shirase Glacier. The colors in the right figure correspond to those in the left figure.

Mid-Holocene deglacial history along the Lützow-Holm Bay verified by the geodetic observations and GIA modeling

Akihisa Hattori[1], Jun'ichi Okuno[1,2,3], Koichiro Doi[1,3], Yuichi Aoyama[1,3]
[1]*Department of Polar Science, The Graduate University for Advanced Studies, SOKENDAI*
[2]*Research Organization of Information and Systems*
[3]*National Institute of Polar Research*

The Antarctic ice sheet variation deforms the solid Earth at various spatial and temporal scales. In particular, the viscoelastic deformation caused by the ice sheet melting since the Last Glacial Maximum (LGM), generally called the glacial isostatic adjustment (GIA), is essential to estimate the current Antarctic ice mass change precisely. Geodetic surveys are vital in constraining and calibrating the GIA models by measuring the recent crustal deformation.

Japan Antarctic Research Expedition (JARE) has been conducting GNSS observations along the coast of the Lützow-Holm Bay for more than 20 years to monitor the GIA crustal motion. Hattori et al. (2021) revealed that the uplift rates observed at these GNSS sites are inconsistent with the predicted velocities of conventional GIA models (e.g., ICE-6G: Argus et al., 2014) and suggested that conventional ice sheet history models do not represent the actual local ice sheet history sufficiently. Kawamata et al. (2020) reported from geographical surveys in Skarvsnes, one of the outcrop sites along the coast of Lüutzow-Holm Bay, experienced more than 400 m of ice sheet melting between 9 and 6 thousand years ago by the exposure ages. This rapid ice sheet retreat has not yet been implemented in the conventional GIA models.

In this study, we performed the GIA model calculations using ICE-6G (Argus 2014) model as a reference model and some different settings with changing the timing and amount of ice sheet melting around Lützow-Holm Bay according to Kawamata et al. (2020). Figure 1 shows the time series of ice sheet thickness in the ICE-6G model Lützow-Holm Bay and those in the modified models. Figure 2 summarizes the uplift rates observed by GNSS observations in Hattori et al. (2021) and the predicted values of GIA models at each site using our modified ice sheet melting history. As a result, the GIA predictions based on the modified ice history show better agreement with the geodetic observation values. This result suggests that geodetic observations also detected the rapid ice sheet retreat, as revealed by geographical investigations.

In this presentation, we would like to report these detailed GIA model settings and calculations and compare modeling results with the absolute gravity measurements at Syowa Station.

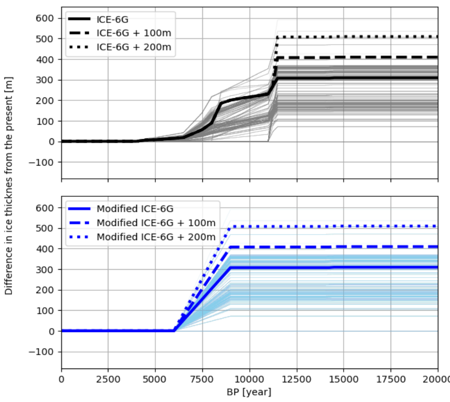

Figure 1 The time series of ice thickness around the Lützow-Holm Bay in ICE-6G and our modified models.

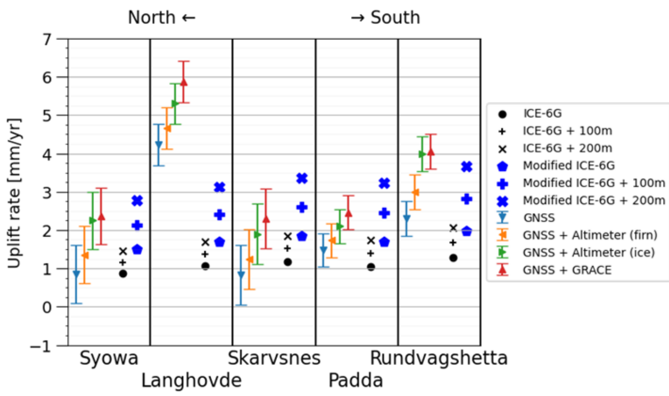

Figure 1 The predicted uplift rate calculated by GIA model and the observed values by GNSS measurements reported by Hattori et al., (2021).

References

Hattori, A., Y. Aoyama, J. Okuno, and K. Doi, GNSS observations of GIA-induced crustal deformation in Lützow-Holm Bay, East Antarctica. Geophysical Research Letters, 48, e2021GL093479, 2021.

Kawamata, M., Y. Suganuma, K. Doi, K. Misawa, M. Hirabayashi, A. Hattori, and T. Sawagaki, Abrupt Holocene ice-sheet thinning along the southern Soya Coast, Lützow-Holm Bay, East Antarctica, revealed by glacial geomorphology and surface exposure dating, Quaternary Science Reviews, 247, 2020.

Argus, D.F., W.R. Peltier, R. Drummond, and A. W. Moore, The Antarctica component of postglacial rebound model ICE-6G_C (VM5a) based upon GPS positioning, exposure age dating of ice thicknesses, and relative sea level histories, Geophys. J. Int., 198(1), 537-563, 2014.